

https://dspace.org/

The effects of ibogaine on myelination in Sprague Dawley rats

Govender, Demi Natisha

2024
University of the Witwatersrand, Johannesburg
https://hdl.handle.net/10539/42966
Govender, Demi Natisha. (2024). The effects of ibogaine on myelination in Sprague Dawley rats [Master's dissertation, University of the Witwatersrand, Johannesburg]. WireDSpace.

Downloaded from a DSpace repository. https://dspace.org/

THE EFFECTS OF IBOGAINE ON MYELINATION IN SPRAGUE DAWLEY RATS



Demi Govender 1444170

SUPERVISORS: DR. TANYA CALVEY, DR. GAVIN OWEN AND DR. NANCY MEULENBERG

Plagiarism Declaration

UNIVERSITY OF THE WITWATERSRAND JOHANNESBURG

FACULTY OF HEALTH SCIENCES

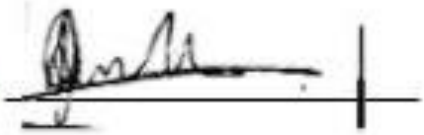
PLAGIARISM DECLARATION TO BE SIGNED BY ALL HIGHER DEGREE STUDENTS

SENATE PLAGIARISM POLICY: APPENDIX ONE

I Demi Natisha Govender (Student number: 1444170) am a student registered for the degree of Msc in Medicine in the academic year 2023.

I hereby declare the following:

- I am aware that plagiarism (the use of someone else's work without their permission and/or without acknowledging the original source) is wrong.
- I confirm that the work submitted for assessment for the above degree is my own unaided work except where I have explicitly indicated otherwise.
- I have followed the required conventions in referencing the thoughts and ideas of others.
- I understand that the University of the Witwatersrand may take disciplinary action against me if there is a belief that this is not my own unaided work or that I have failed to acknowledge the source of the ideas or words in my writing.
- I have included as an appendix a report from "Turnitin" (or other approved plagiarism detection) software indicating the level of plagiarism in my research document.

Signature:  Date: 08/12/2023

Acknowledgments

The first person that I want to acknowledge for providing all their support and encouragement towards not only this masters but to me is my mother, Denise Govender. She has always pushed me to strive for academic excellence and expected nothing less as I started my post graduate journey. I am forever in her gratitude for the kind words, encouraging speeches and constant support. You have been essential in my academic journey.

Secondly, I want to thank my amazing supervisors, Dr. Calvey, Dr. Owen and Dr. Meulenberg, who have not only given me an extensive amount of knowledge and skills but also support and guidance in navigating the rollercoaster that is research from honours to masters. Through all the failed PCRs and western blots, I could always rely on their positivity and discussions around troubleshooting. Although the most guidance came in writing up my thesis, they offered all their expertise to help me become a better academic writer. I want to thank them for giving me the opportunity to grow as a researcher and learn to analyse and describe results in more comprehensive style rather than "Demiing it" as Dr. Owen likes to put it. This has been a memorable experience with many ups and downs and I thank you for helping me through it all.

The next person who needs to be acknowledged is Mrs. Hasiena Ali who spent many afternoons with me rattling through freezers on the second floor. Not only did she go the extra mile to help me with my supplies and lab space but also offered advice and encouragement when the results were not what I expected. Mrs. Ali is truly an amazing mentor to any post graduate student with heaps of advice and knowledge.

Lastly, I want to thank all my family for all their encouragement and support because without all of them I would not have been able to make it through all the highs and lows of research within the craziness of a pandemic. A special thanks to my sisters for putting up with all the random outbursts of theories I sprouted on them, my brother-in-law for being my personal uber for rat injection days, my niece and nephew for always being rays of sunshine to brighten any bad lab day and my boyfriend who put up with all the stress outbursts, random rantings when experiments failed and for the endless encouragement he offered.

Table of Contents

Plagiarism Declaration i

Acknowledgments ii

Table of Figures iv

List of Abbreviations vi

Abstract 1

1. Introduction: Literature Review 3

1.1 Drug Addiction: The History and Neurobiology 3

1.1.1 The Neurobiology of Opioid Addiction and Hyperkatifeia 6

1.2 The Opioid Crisis and its impact in South Africa 7

1.3 Psychedelics and addiction therapy 9

1.3.1 Ibogaine as a possible aid in addiction therapy 11

1.4 White matter of the Brain and the effects of opioid addiction 13

2. Aim and Objectives 15

3. Methods 16

3.1 Saline, Ibogaine and Chronic Morphine Administration to Sprague Dawley Rats 16

3.1.1 White Matter Tissue collection from the Sprague Dawley Rat Brains 17

3.2 White Matter Sample preparation for qPCR and Western Blotting 19

3.3 Bicinchoninic Acid (BCA) Assay of Total Proteins Extracted from White Matter 20

3.4 Reverse Transcription of Extracted mRNA from white matter into cDNA 20

3.5 Optimisation of Quantitative Polymerase Chain Reaction (qPCR) protocol for the cDNA from the White Matter of SD rats 20

3.5.1 The Pfaffl Method for analysis of qPCR data 22

3.6 SDS PAGE of the White Matter Total Protein from SD Rats 23

3.7 Western blotting and immunofluorescence of the White Matter Samples 24

4. Statistical analysis 25

5. Results....26

5.1 An immediate increase in mRNA fold expression of CNP after chronic morphine administration followed by ibogaine....26

5.2 Ibogaine administration after chronic morphine regimen increases CNPase protein expression 3 days post-administration in Sprague Dawley Rats....28

5.3 Ibogaine decreases MBP fold expression of mRNA in Sprague Dawley rats when administered alone....30

5.4 Increased MBP (18,5 kDa) protein expression after ibogaine administration....31

5.5 Increased expression of PLP gene in ibogaine treated rats and decreased expression in chronic morphine rats with an increased protein expression of PLP in 3-day post ibogaine and chronic morphine treated rats....33

6. Discussion....35

References....40

Table of Figures

Table 1: The framework of addiction with relation to functional areas, neurocircuitry and neurotransmitters (Koob and Moal, 2005; Koob and Volkow, 2016; Shurman *et al.*, 2010; Uhl *et al.,* 2019)....6

Table 2: Primers for genes used in qPCR (CNP, MBP, PLP and beta actin)....21

Figure 1: Neurobiology of the addiction cycles....5

Figure 2: The Neuroplastic Effects of Psychedelics at Various Levels of the Brain....10

Figure 3: Structure of Myelin and its associated proteins....15

Figure 4: Morphine and Ibogaine Treatment Schedule for Sprague Dawley rats. The morphine and ibogaine treatments given to the (SD) rats....18

Figure 5: Agarose gel of CNP, PLP and MBP Primers tested at 51°C.....22

Figure 6: Relative expression of CNP gene shows an immediate increase in mRNA expression of CNP after ibogaine administration following chronic morphine administration....27

Figure 7: A-Peak density measurements and B- representative western blots of CNP protein expression of white matter in SD rats showed increased expression in morphine ibogaine treatment after a 3 day wait and in the morphine control group.....29
Figure 8: Relative mRNA expression of MBP is decreased after ibogaine administration.....30
Figure 9: Peak density of MBP in white matter of the SD rats showed increased MBP expression after ibogaine administration.....31
Figure 10: Representative western blots showing 21,5 kDa and 18,5 kDa isoforms of MBP. The immunoblots show the MBP probed samples with their corresponding β-actin probed samples. 32
Figure 11: Relative Fold expression (9A) and peak density (9B) of PLP1 from qPCR and western blots of white matter of SD rats shows increase in morphine ibogaine groups.. 34
Figure 12: Representative western blots of the white matter from the SD rats probed for PLP. These immunoblots show the PLP probed samples with their corresponding β-actin probed sample.....34

List of Abbreviations

BCA	Bicinchoninic Acid
BDNF	Brain Derived Neurotrophic Factor
BSA	Bovine Serum Albumin
CNP	2', 3’-cyclic nucleotide 3'-phosphodiesterase (CNPase)
CNS	Central Nervous System
DAT	Dopamine Transporter
DMT	N, N-dimethyltryptamine
DNA	Deoxyribonucleic Acid
GABA	γ-aminobutyric acid
GDNF	Glial Derived Neurotrophic Factor
ip	intraperitoneal
LSD	lysergic acid diethylamide
MBP	Myelin Basic Protein
MDMA	3,4-methylenedioxymethamphetamine
mRNA	Messenger Ribonucleic Acid
NMDA	N-methyl-D-aspartate
OPC	Oligodendrocyte Progenitor Cells
PAP	Psychedelic-Assisted Psychotherapy
PBS	Phosphate Buffered Saline
PCP	phencyclidine
PCR	Polymerase Chain Reaction
PLP	Proteolipid Protein
PTSD	Post traumatic stress disorder
qPCR	Quantitative Polymerase Chain Reaction
RT-PCR	Reverse Transcription Polymerase Chain Reaction
sc	Subcutaneous
SD	Sprague Dawley
SDS	Sodium Dodecyl Sulphate
SDS-PAGE	Sodium Dodecyl Sulphate Polyacrylamide Gel Electrophoresis
SERT	Serotonin Reuptake Transporters

SUD	Substance Use Disorder
TBS	Tris Buffered Saline
THC	tetrahydrocannabinol
VTA	Ventral Tegmental Area

Abstract

Introduction: The growing opioid epidemic is a worldwide issue which is prevalent in South Africa with the use of opioid cocktails such as nyaope. A possible solution to this problem is the use of psychedelic assisted psychotherapy. Ibogaine is a psychedelic that has been shown to curb addiction cravings and have neuroplastic effects in the brain. Ibogaine is extracted from the root bark of a West African plant and has shown to have neuroplastic effects in the brain. We investigated whether these antiaddictive properties are due to remyelination of the brain's white matter.

Methods: This study uses qPCR and western blotting to determine how myelin specific proteins and genes such as CNPase (CNP), Myelin Basic Protein (MBP) and Proteolipid Protein (PLP) are affected by morphine (opioids) and ibogaine. The experimental rat groups included a saline, morphine and ibogaine only controls, a combination morphine and ibogaine and a second combination morphine and ibogaine which included a 3 day withdrawal after ibogaine injection.

Results: CNP protein was increased in the second morphine ibogaine group ($p<0,0001$) and the CNP mRNA fold expression was increased in the first morphine ibogaine group compared to the second morphine ibogaine group ($p=0,0343$). The 18,5 kDa isoform of MBP had increased expression in the ibogaine control ($p=0,0384$) and second morphine ibogaine group ($p=0,0037$). PLP shows increased protein expression in the second morphine ibogaine group when compared to the first group ($p=0,0464$). There is decreased PLP mRNA expression in the ibogaine control group when compared to morphine control ($p=0,0033$), first morphine ibogaine ($p<0,0001$) and second morphine ibogaine groups ($p=0.003$)

Conclusion: Ibogaine may cause remyelination following demyelination by morphine. A consistent trend in the data shows that the myelin proteins were increased after the 3 days after administration of ibogaine following chronic morphine administration compared to 1 day after administration of ibogaine. This suggests that remyelination takes between 24-72 hours before it begins to produce new myelin around the axons due to ibogaine. These results also shows that CNP and MBP increase in expression earlier than PLP and are good markers for early remyelination. This is consistent with increase in CNP mRNA expression for CNP seen

in the first morphine ibogaine but not the second group revealing an immediate effect on mRNA but a delay in protein expression.

1. Introduction: Literature Review

1.1 Drug Addiction: The History and Neurobiology

Drug addiction or substance use disorder is a chronically relapsing disorder characterized by three characteristics: compulsive seeking and use of the drug, a lack of control to limit the use of the drug, and a negative emotional state resulting from withdrawal of the drug such as irritability, anxiety or paranoia (Koob and Le Moal, 2008). Although the DSM-V criteria for substance use disorder (SUD) is divided into 4 main categories: impaired control, physical dependence, social problems and risky use (Nathan *et al.,* 2016).

Addiction has been documented as early as 323BC after Alexander the Great's death due to heavy drinking. Aristotle and Celsus recorded signs of withdrawal and dependence following excessive alcohol use. China in the 18th century showed the addictive properties of opium as the government tried to limit sales and consumption due to the rise in use from Chinese people (Crocq, 2007a). The introduction of the Journal of Addiction in Britain and Journal of Inebriety in America in the 19th century allowed for research to be consolidated and become more widely available. This encouraged more research on addiction by scientists (Crocq, 2007a; Nathan *et al*., 2016) which led to the 20th century diagnostic classifications and medical research boom. Only in 1924 did addictive substances become categorised by Louis Lewin. This categorisation included stimulants such as caffeine or nicotine, inebriants, hallucinogens, euphoriants such as opium or cocaine and hypnotics. This allowed for better understanding of how each category affected the individual and caused addiction. Animal research allowed for a better understand of how addiction affected the rewards system of the brain and allows for conditioning, which is when the brain relates the use of the substance to a reward (Crocq, 2007a).

The effects of addiction in the brain is better understood now than in the 19th century when it was first introduced as a concept in medicine (Crocq, 2007a). The neurobiological aspects have been studied in both human and animal studies that have allowed us to better understand the neurochemical and neurobiological changes associated with addiction. This is characterised by the heuristic framework which outlines a continuous three stage cycle that includes: a binge and intoxication phase, withdrawal phase and anticipation phase (Koob and Volkow, 2016). This framework will guide us through the neurobiology of addiction.

The binge phase highlights the dysregulation of incentive salience which are the habits of the person. Incentive salience occurs via conditioned reinforcement of drug seeking behaviour to a specific stimulus that was once neutral (Koob and Moal, 2005; Uhl *et al.,* 2019). Dopamine plays a critical role in this phase of addiction. The general understanding is that addictive substances increase the brains' dopamine. This is within the nucleus accumbens which plays a vital role in the reward system of the brain as seen in table 1 under neurocircuitry. This dysregulation affects the dopamine receptors namely D1 and D2 receptors. The increased dopamine mimics phasic firing of dopamine neurons which is normally only present during extremely rewarding or adverse events (Saal *et al.,* 2003). This activates both D1 and D2 receptors. The D1 receptors stimulate pathways to the striatum and cortex but the interesting pathway is to the amygdala, orbitofrontal cortex and hippocampus which are responsible for conditioning and memory as seen in figure 1. The D2 receptors modulate the effects of D1 via the indirect striatal pathway but in an addicted brain there are fewer D2 receptors. This impaired signalling and increased dopamine in the prefrontal and orbitofrontal areas result in compulsive and impulsive behaviours, signalling of incentive salience of events, drives motivated behaviour, affects the prediction of reward and non-reward stimuli and facilitates consolidation of memory for salient events (Koob and Moal, 2005; Diana, 2011; Koob and Volkow, 2016). Increased serotonin affects behavioural inhibition, emotional stabilization, sensory reactivity and pain sensitisation. Along with serotonin, dopamine, γ-aminobutyric acid (GABA), opioid peptides and acetylcholine shown in table one also act on the dorsal striatum and VTA to increase incentive salience and dysregulate the stress, reward, motivation and memory circuits in the brain (Koob, 2008; Koob and Le Moal, 2008).

Withdrawal from chronic administration of drugs results in many negative effects. This includes irritability, anxiety, depression, elevated stress and emotional dysregulation. The brain stress system is recruited during withdrawal as pro-stress neurotransmitters such as corticotropin-releasing factor (CRF), norepinephrine (NE) and dynorphin are increased and antistress neurotransmitters such as neuropeptide Y, oxytocin and endocannabinoids are decreased (Koob, 2008; Koob and Le Moal, 2008) as shown in table 1. Norepinephrine acts on two ascending pathways from the dorsal noradrenergic bundle in the locus coeruleus of the brainstem where it is produced to the hippocampus, cerebellum and forebrain and from the nuclei of the pons and medulla to the hypothalamus, midbrain and extended amygdala shown

in figure 1 (Koob, 2008; 2020). These cause an increased sensitivity to stress. In the nucleus accumbens, serotonin and dopamine transmission is decreased (Volkow *et al.,* 2007; Weiss *et al.,* 1992). There is also a decrease in GABA transmission and an increase in glutamatergic NMDA transmission in the nucleus accumbens. In combination, these result in a decreased functioning of the reward system and increased functioning of the brain stress system. This dysfunction leads to cravings for the addictive substance as normal activities do not create the same feeling of reward.

Anticipation is the craving for the addictive substance. This is said to be the biggest reason for relapse in patients who suffer from addiction (Koob and Le Moal, 2008; Koob and Volkow, 2016). This phase incorporates the low functioning reward system and high stress response to cause drug seeking behaviour. The main neurobiological cue for this stage is the glutamatergic projection from the amygdala to the nucleus accumbens and prefrontal cortex connections (Everitt and Wolf, 2002; Koob and Le Moal, 2008; Weiss *et al.,* 2001) as shown in table 1 and figure 1. The increased stress hormones such as CRF and orexin are triggered in stressful situations which can cause drug seeking behaviour and cause relapses (Koob, 2008).

Binge and Intoxication

- Increase in dopamine in Ventral Striatum (VS) which includes nucleus accumbens
  - Euphoria and reward
- Dorsal striatum, globus pallidus and thalamus
  - Habits and preservation (incentive salience)

Withdrawal

- Extended amygdala (amygdala (AMG) and bed nucleus of stria terminalis (BNST))
  - Negative emotional state by brain stress system recruiting pro-stress neurotransmitters
  - Specifically, norepinephrine which causes increased reactivity to stress
- Ventral striatum (VS)
- Decreased reward due to decreased dopamine and serotonin transmission

Anticipation

- Main cue: Glutamergic projection from amygdala (AMG) to nucleus accumbens in VS and prefrontal cortex (mPFC)
  - Effects of craving and dysfunction of executive function
- Hippocampus and basolateral nucleus of the AMG
  - Conditioned cues

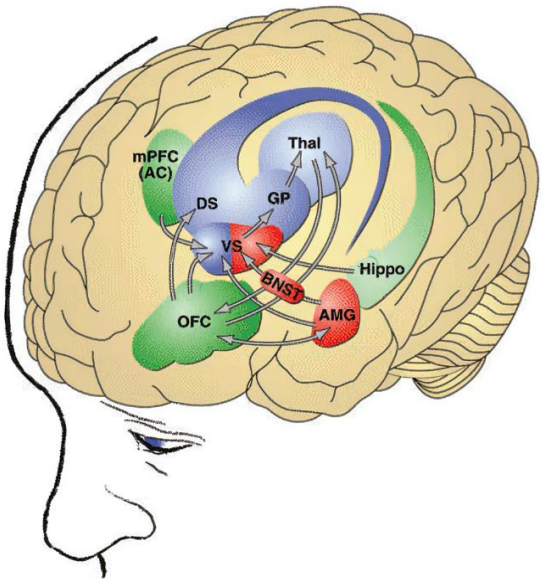


Figure 1: Neurobiology of the addiction cycles (Koob, 2010)

Table 1: The framework of addiction with relation to functional areas, neurocircuitry and neurotransmitters (Koob and Moal, 2005; Shurman *et al*., 2010; Koob and Volkow, 2016; Uhl *et al.,* 2019)

Heuristic Framework of Addiction	**Dysregulation in these Functional Domains**	**Major Neurocircuitry that is affected**	**Neurotransmitters affected**
Binge and Intoxication	Incentive salience Motivation and Reward	• Basal ganglia-Specifically dorsal striatum • Ventral Tegmental Area (VTA)	Dopamine (↑) Opioid peptides (↑) Serotonin (↑) GABA (↑) Acetylcholine (↑)
Withdrawal (negative effect)	Negative emotional state	• Extended amygdala (central nucleus and bed nucleus of stria terminalis) • Habenula • Shell of nucleus accumbens • VTA	**Increased stress neurotransmitters:** Corticotropin-releasing factor (↑) Norepinephrine (↑) Dynorphin (↑) Orexin (↑) **Decreased antistress neurotransmitters:** Neuropeptide Y (↓) Oxytocin (↓) Endocannabinoids (↓) Dopamine (↓) Serotonin (↓)
Preoccupation and anticipation	Executive function	• Prefrontal cortex • Hippocampus • Basolateral amygdala • Lateral bed of stria terminalis • Insula	Dopamine (↑) Glutamate (↑) Orexin (↑) Serotonin (↑) Corticotropin-releasing factor (↑)

1.1.1 The Neurobiology of Opioid Addiction and Hyperkatifeia

Opioid addiction follows the heuristic three stage cycle of addiction: intoxication, withdrawal and anticipation with it worsening due to continuous drug use (Koob, 2020). Chronic opioid administration induces neurochemical changes that alter brain systems and circuits namely the reward circuit to decrease the reward sensation and the brain stress system to increase stress and compulsivity. Opioids differ from most substance addictions as negative

reinforcement usually starts and drives the cycle (Koob, 2020). The opponent process theory is important to understand in opioid addiction as it shows that positive feelings (euphoria) is followed by a negative state (dysphoria). As opioids are used the negative sensations become larger and the euphoria lessens (Koob *et al.,* 1989). The repeated stages of intoxication and withdrawal lead to hypohedonia which is a reduced ability to experience pleasure or reward, hyperkatifeia is a hypernegative emotional state, hyperalgesia and increased negative behavioural responses to stress (Koob *et al.,* 1989).

Hyperkatifeia occurs during opioid withdrawal where the extracellular dopamine is decreased in the nucleus accumbens (Pothos *et al.,* 1991) and mesolimbic dopamine systems which decreases dopamine neuron firing (Diana, 2011; Rossetti *et al.,* 1992). This occurs with an increase in GABA and metabotropic glutamate release in the VTA which also results in decrease dopamine neuron firing (Bonci and Williams, 1997). Chronic morphine administration decreases the size of dopamine neurons in the VTA and increases the sensitivity of dopamine receptor antagonists (Bonci and Williams, 1997). Hyperalgesia is a decrease in pain threshold or tolerance. This causes an increased sensitivity to pain and becomes a driving factor in drug seeking behavior. The activation of the glutamatergic systems and brain stress system are the mechanisms for opioid induced hyperalgesia (Célèrier *et al.,* 2001; Compton *et al.,* 2001; Laulin *et al.,* 1998). Hyperalgesia and hyperkatifeia are side effects of the activation of brain stress system which employs CRF and dynorphin. Two important structures that facilitate hyperalgesia and hyperkatifeia are the periaqueductal gray (PAG) and lateral habenula. The PAG processes pain and is important in the development of tolerance to opioids. It does this by increasing the gene expression of proinflammatory factors and increasing glutamatergic tone of the neurons (Eidson *et al.,* 2017; Eidson and Murphy, 2013; George *et al.,* 2019; Wang *et al.,* 2012). The lateral habenula is a connection to the brain reward system. It inhibits the dopamine neurons in the VTA which has been observed in humans by increased connectivity between the habenula and striatum of opioid addicts (Curtis *et al.,* 2017).

1.2 The Opioid Crisis and its impact in South Africa

Addiction is an international public health crisis but in the last few years the rise in opioid addiction has caused extreme concern. Although the opioid crisis began in China, America had an increased spike in opioid addiction in the late 1900s. This spike was caused by a few

factors as described by Weiner *et al*., 2017: pain management being declared a human right as of the Montreal Declaration in 2010, a physicians' obligation to treat pain more aggressively thus prescribing opioids which was spearheaded by the perception of under treated pain and lastly the exponential increase of marketing of opioids for pain management by the pharmaceutical industry. All these escalated the world health crisis of opioid addiction.

Although the sudden rise of opioid addiction has shocked the world, its highly addictive nature and the difficulty in treating the addiction has been evident for centuries (Crocq, 2007b; Vadivelu *et al.,* 2018). Opioids were first used as early as the 9th century to treat injured soldiers but during the 18th century opium was used to treat depression-like syndromes (Crocq, 2007b; Harker *et al.,* 2020; Nathan *et al.,* 2016; Vadivelu *et al*., 2018). The addictive quality of opioids were first identified in China when people showed signs of addiction (Crocq, 2007b). The government implemented regulatory laws to counteract this (Crocq, 2007b; Harker *et al*., 2020; Vadivelu *et al.,* 2018). In South Africa opioids were mainly available to the white middle-class in the forms of heroin and the injectable opioid, Wellconal (Harker *et al.*, 2020; Pliiddemann *et al.,* 2008). This developed into lower grade heroin being mixed into drug cocktails and branching into the poorer communities as it was cheaper and highly addictive (Chetty *et al.,* 2020; Harker *et al*., 2020; Khine *et al.,* 2016).

There has been a rise in opiate use in Africa (Kurth *et al.,* 2018; Ndlovu *et al.,* 2021). Sub-Saharan Africa is one of the three regions in the world with the highest rates of opioid-related premature mortality and in South Africa, heroin is the most abused opioid (Ndlovu *et al.,* 2021). Although opioid addiction seemed to be a first world problem, the use of African trade routes to traffic opioids has increased the rate of consumption in the continent (Harker *et al.,* 2020; Kurth *et al.,* 2018). Opioids are used in common South African street drug cocktails such as nyaope in Gauteng, sugars in KwaZulu Natal, pinch in Mpumalanga and whoonga or unga in the Western Cape (Chetty *et al.,* 2020; Khine *et al.,* 2015, 2016). These are all highly addictive and have other additives in them such as cocaine, cannabis, amphetamines and anti-retrovirals (Khine *et al.,* 2015, 2016). The street names for these cocktails have misled the public from seeing the rising opioid abuse epidemic in South Africa (Chetty *et al*., 2020).

Over the past 20 years, there has been a steep rise in opiate addiction treatment admissions in South Africa (Harker *et al.,* 2020; Peltzer *et al.,* 2011) although patient retention and

treatment outcomes are poor reflecting inadequate treatment services for those affected by opioid dependence (Morgan and Wang, 2019). The driving factor to this increase in opioid addiction in South Africa is the emergence of the drug cocktail, nyaope (Harker *et al.,* 2020). Nyaope has been the most researched of the drug cocktails available in South Africa showing that it primarily consists of marijuana and a form of opioid either heroin or morphine (Khine *et al.,* 2015; Mthembi *et al*., 2018). One of the alarming findings from composition studies of nyaope is that it contains methadone which is generally used to treat addiction and curb cravings (Khine *et al.,* 2015, 2016; Mthembi *et al.,* 2018). Alternative therapies to help treat the addiction and cravings such as Buprenorphine and Naltrexone will not be effective as they are opiate receptor antagonists and due to the cannabis upregulating opiate receptors in the brain when combined with chronic opioid administration (Cichewicz, 2004; Cichewicz *et al.,* 2001). These treatments will not be effective for these drug cocktails which are mainly opioids and cannabis (Khine *et al.,* 2016). There is a growing need for intervention and alternative treatment for opioid addiction especially with drug cocktails such as nyaope being widely available and relatively cheap. This need is evident as there is an increase in alternative medicine being used to treat opioid addiction and depression (Ndlovu *et al.,* 2021).

1.3 Psychedelics and addiction therapy

Psychedelics are psychoactive compounds that can be divided into two categories: classical and non-classical psychedelics. Classic psychedelics are direct agonists of serotonin receptors such as lysergic acid diethylamide (LSD), N, N-dimethyltryptamine (DMT), psilocybin and mescaline (Barsuglia *et al.,* 2018a; Calvey and Howells, 2018; Mendes *et al.,* 2022). Non-classical psychedelics vary in their mechanism of action and pharmacological properties but are generally classified under four categories: dissociative psychedelics which are NMDA antagonists such as ketamine, phencyclidine (PCP) and ibogaine, cannabinoid agonists such as tetrahydrocannabinol (THC), muscarinic receptor antagonists such as scopolamine and entactogens such as 3,4-methylenedioxymethamphetamine (MDMA) (Calvey and Howells, 2018).

Psychedelic research boomed in the 1950s to 1970s but due to stricter laws and psychedelics becoming illegal or controlled substances it became less widely available to study (Belouin and Henningfield, 2018; Mendes *et al.,* 2022). During the psychedelic research boom it was discovered that SUDs could be treated with psychedelics to reduce cravings and manage the

depression and anxiety commonly associated with it (Bogenschutz *et al.,* 2018; Calleja-Conde *et al.,* 2022; Chi and Gold, 2020; Das *et al.,* 2016; Mash *et al.,* 1998; Peltz and Südhof, 2018). This led to rehabilitation centres beginning to make use of psychedelic assisted therapies during the recovery process.

Psychedelic-assisted psychotherapy (PAP) for psychiatric disorders such as depression, PTSD, bipolar disorder and addiction has become more widely available with clinical trials and psychedelic treatment programmes in psychiatric facilities. Psychedelics act on the serotonergic and dopaminergic systems which are generally affected by these disorders (Aleksandrova and Phillips, 2021; Belouin and Henningfield, 2018; Calleja-Conde *et al.,* 2022; Chi and Gold, 2020; Glick and Maisonneuve, 1998). They have shown to have fast acting and long-term effects (Aleksandrova and Phillips, 2021; de Vos *et al.,* 2021; Mendes *et al.,* 2022). These psychedelics generally work through the $5HT_{2A}$ or NMDA receptors to increase cortical glutamate release (De Gregorio *et al.,* 2018; Kadriu *et al.,* 2021; Razoux *et al.,* 2007). This signalling pathway causes changes in gene expression or transcription such as mTOR, BDNF (brain-derived neurotrophic factor) and GDNF (glial-derived neurotrophic factor) which leads to structural changes on a cellular level as depicted in figure 2. This cascade effects is what causes the neuroplastic changes seen with psychedelics (Figure 2) (Aleksandrova and Phillips, 2021; de Vos *et al.,* 2021; Ly *et al.,* 2018; Marton *et al*., 2019).

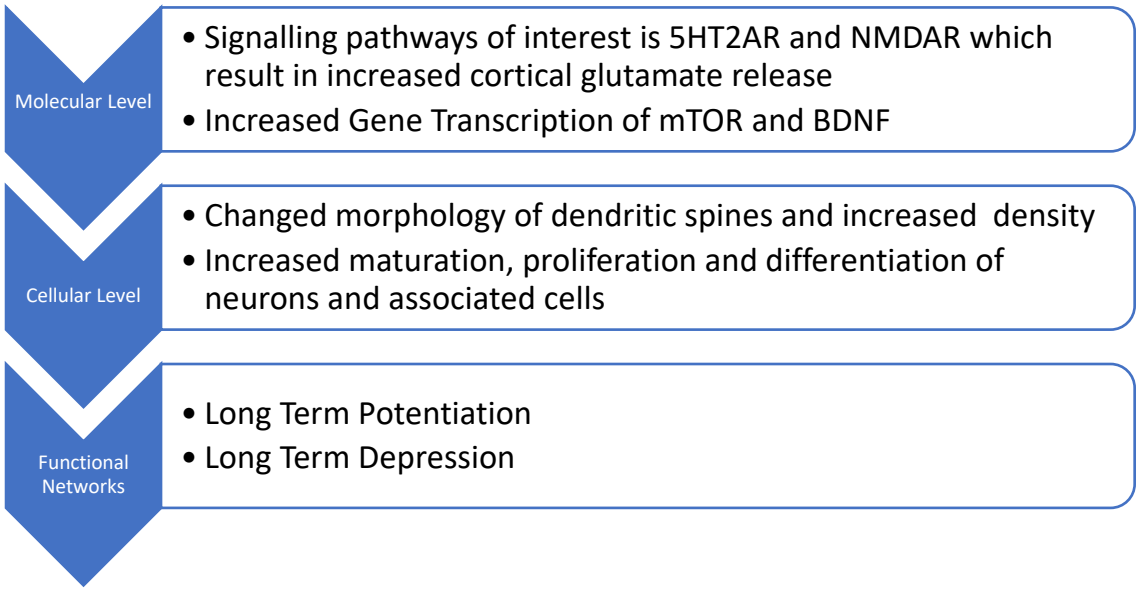


Figure 2: The Neuroplastic Effects of Psychedelics at Various Levels of the Brain (Adapted from de Vos *et al*., 2021; Kelmendi *et al.,* 2022)

1.3.1 Ibogaine as a possible aid in addiction therapy

Ibogaine is an indole alkaloid found in the root bark of the iboga shrub, which is native to West Africa (Alper, 2001). It is classified as an atypical dissociative psychedelic (Calvey and Howells, 2018). Iboga shrubs have been used in traditional medicine for thousands of years during ancestral communication rituals (Barsuglia *et al.,* 2018c; Calvey and Howells, 2018) . Ibogaine can be used from the root bark or as a salt, ibogaine HCl *(*Alper*,* 2001; Barsuglia *et al.,* 2018a). The bark contains other alkaloids such as ibogaline, ibogamine, and tabernanthine (Bouso *et al.,* 2020).

The mechanism of action for ibogaine is unique due to the complexity of a multiple receptor profile (Alper, 2001). The generally accepted mechanism of action is that ibogaine acts on many neurotransmitter systems within the brain (Barsuglia *et al.,* 2018, 2018). The receptor affinities identified for ibogaine are mμ-opioid and kappa-opioid receptors, Sigma 1 and Sigma 2 receptors, serotonin reuptake transporters (SERT), dopamine transporter (DAT), α3β4 nicotinic acetylcholinergenic receptor and the N-methyl-D-aspartate (NMDA) receptor (Barsuglia *et al.,* 2018a; Brown and Alper, 2018; Mash *et al.,* 1998). This has shown to produce an overall effect of dopamine reduction in the brain with an increase in dopamine breakdown (Glick *et al*., 2001). Ibogaine needs to be metabolised by the CYP_{2D6} liver enzyme into its active metabolite noribogaine. Noribogaine then acts on receptors and stays within the system for long lasting effects.

Ibogaine gained attention in western medicine during the 1960s, when it was identified to reduce cravings for addictive substances such as alcohol, methamphetamines, cocaine, nicotine and opiates (Alper, 2001; Barsuglia *et al.,* 2018c; Brown and Alper, 2018). The anti-addictive properties of ibogaine are utilized in rehabilitation clinics locally and internationally according to the Global Ibogaine Therapy Alliance (GITA) consensus clinical treatment guidelines for screening and risk management (Barsuglia *et al.,* 2018a). Ibogaine has been legalized and controlled in countries such as South Africa, Uruguay, New Zealand, Hungary, Denmark, Canada, Brazil and Australia (Barsuglia *et al.,* 2018b). There have been studies that showed cerebellum neurotoxicity specifically in purkinje cells due very high doses of ibogaine (>100 mg/kg) which is not used in treatment protocols. These neurotoxic effects are suggested to be species specific as Alper (2001) identified differences in studies between monkeys, rats and mice. Another major issue seen with ibogaine use is that there are some

cardiovascular risks as it can decrease the heart rate of participants, but this is also only seen in high doses of ibogaine (>100 mg/kg). Cardiac screening before ibogaine administration is important to prevent cardiac risk. Research is needed on ibogaine to understand its complex mechanism of action, formulate treatment for addiction in medical practice and the possibility of it being used for non-addictive pain management of chronic pain disorders.

Ibogaine can eradicate drug cravings (Barsuglia *et al.,* 2018) although the neuropharmacological mechanism of how it is able to do so remains largely unknown. It is suggested that ibogaine can elicit large-scale neuroplastic effects in the brain (Barsuglia *et al.,* 2018c; de Vos *et al.,* 2021; Du *et al.,* 2006a; Marton *et al.,* 2019). Ibogaine has thus been termed a psychoplastogen (Ly *et al.,* 2018), as it promotes cell survival, is neuroprotective and can modulate the neuroimmune system of the brain amongst other neuroplastic effects (Calvey and Howells, 2018). Further research is required to understand its complex mechanism of action. Recent findings in our lab suggest that ibogaine can increase myelination following chronic morphine exposure (Govender *et al.,* 2020).

Ibogaine has a reversible voltage gated antagonistic effect on NMDA receptors (Popik *et al.,* 1994). The NMDA receptor antagonistic properties of ibogaine should induce interesting effects on the oligodendrocytes of the central nervous system (Glick and Maisonneuve, 1998; Lundgaard *et al*., 2013). The NMDA receptors present on oligodendrocytes regulate myelination and axonal health (Saab *et al.,* 2016). NMDA receptor activation increases myelination and CNPase by increasing the cytosolic calcium and reactive oxygen species (Cavaliere *et al.,* 2012). Due to ibogaine's voltage gating the cytosolic calcium will need to be at lower levels to activate the NOX-dependent generation of reactive oxygen species, which will activate the PI3K/AKT pathway (Cavaliere *et al.,* 2012). The PI3K pathway promotes neural plasticity and improves memory by activating mTOR. This pathway could also be affected directly by ibogaine as mTOR gene expression is upregulated by noribogaine which is the principal metabolite of ibogaine (Ly *et al.,* 2018).

The sigma 1 receptor agonist affinity of ibogaine could also affect the oligodendrocytes CNPase activity, as the sigma 1 receptor regulates Ca2+ channels, which is important for CNPase activity and regulation of gene expression (Soriani and Kourrich, 2019). It also increases BDNF and GDNF, which has been shown to have neuroplastic effects in addiction

(Carnicella and Ron, 2009; Marton *et al.,* 2019). The kappa opioid receptor has been implicated in increasing oligodendrocytes thus increasing remyelination in the CNS (Mei *et a*l., 2016). This can be another way in which ibogaine affects oligodendrocytes as it is a kappa opioid agonist (Glick *et al.,* 1997).

1.4 White matter of the Brain and the effects of opioid addiction

The white matter of the brain is composed primarily of oligodendrocytes, astrocytes and the myelinated axons of neurons. Myelin is a major component of white matter which gives the white matter its characteristic white colour. White matter forms tracts to connect different parts of the brain. The oligodendrocytes are the myelin producing cells of the central nervous system (CNS), they cover the axons to form concentric layers of myelin. Although, this may not be the only function of the oligodendrocytes as evidence suggests a metabolic support role to the axons (Fünfschilling *et al.,* 2012).

Oligodendrocytes have been understudied with regards to drug abuse and its effects (Miguel-Hidalgo, 2018) but the effect of opioid addiction is associated with demyelination (Fan *et al.,* 2018; Liu *et al.,* 2013). Liu *et al*., (2013) found demyelination occurred in chronic heroin users, which supports the evidence that morphine decreases myelin in white matter (Fan et al., 2018). Upadhyay *et al.,* (2010) showed decreased anisotropy in MRIs of white matter tracts specifically in the amygdala-specific tracts which suggests decreased white matter tract connectivity in brains affected by chronic opioid abuse. This further suggests that opioid addiction causes demyelination. There are three myelin markers that have commonly been used to assess the amount of myelin present in a sample: myelin basic protein (MBP), proteolipid protein (PLP) and CNPase (CNP) protein. Changes in expression and abundance of these proteins can be used as markers for increased or decreased myelin (Oberoi *et al.,* 2019). MBP, CNP and PLP are good early markers for remyelination as shown by Lindner *et al.,* 2008.

Myelin basic protein (MBP) is the second most abundant myelin sheath protein and has four main isoforms which are 21.5 kDa, 18.5 kDa, 17 kDa and 14 kDa (Akiyama *et al.,* 2002). It compromises 30% of the total myelin protein and is a structural protein that is essential for CNS myelin (Boggs, 2006). It is bound to the cytosolic membrane of the oligodendrocytes as seen in figure 3 between the layers of cells. It is involved in the adhesion of the cytosolic surface of the myelin sheath layers (Boggs, 2006; De Vries *et al.,* 1997). Therefore, its main

function is adhesion for the myelin sheath formation and has a critical role in myelination or remyelination. The 18.5 kDa MBP is considered to be the classic MBP as this is what most papers refer to when discussing MBP and its functions and is the MBP isomer that is the most prevalent in the adult brain (Boggs, 2006; Harauz and Boggs, 2013). Classic MBP is produced just before the axon is covered in myelin and is important for the membrane adhesion and the cytoskeletal structure of myelin (Boggs, 2006; Harauz and Boggs, 2013). The 21.5 kDa MBP is the first MBP isomer to be synthesized by oligodendrocyte progenitor cells (OPCs) during myelination (Harauz and Boggs, 2013) and is important during early myelination as it has been implicated in differentiation of the cells (De Vries *et al.,* 1997; Jordan *et al.,* 1990; Pedraza *et al.,* 1997) and in remyelination (Capello *et al.,* 1997). It increases oligodendrocyte proliferation and secretion of soluble factors such as Neurotropic growth factor (NGF) and brain derived growth factor (BDNF)(Capello *et al.,* 1997).

CNPase (2', 3'-cyclic nucleotide 3'-phosphodiesterase) is an enzyme and structural protein present in the cytoplasm of oligodendrocytes that catalyses the hydrolysis of 2',3'-cyclic nucleotides (Verrier *et al.,* 2013). It makes up 4% of the myelin proteins in the (Verrier *et al.,* 2013). It is needed during the early stages of oligodendrocyte differentiation and has been associated with compacting the myelin layers on axons as it is seen on the outer layers of the cells in figure 3 (De Vries *et al*., 1997; Maier *et al.,* 2008). Proteolipid protein (PLP) is a 30 kDa hydrophobic membrane protein in CNS myelin and compromises 50% of the total myelin proteins which makes it the main component of myelin proteins (Laule *et al.,* 2007). The main function of PLP is to adhere the myelin lamellae together and create compact concentric layers to increase the stability of the myelin. This is shown in figure 3 as PLP runs from the cytoplasm outwards to the membrane (Ruskamo *et al.,* 2022). Figure 3 depicts the arrangement of these myelin proteins within the myelin sheath (Laule *et al*., 2007). Changes in expression and abundance of these proteins can be used as markers for increased or decreased myelin (M. Lindner *et al.,* 2008; Oberoi *et al.,* 2019).

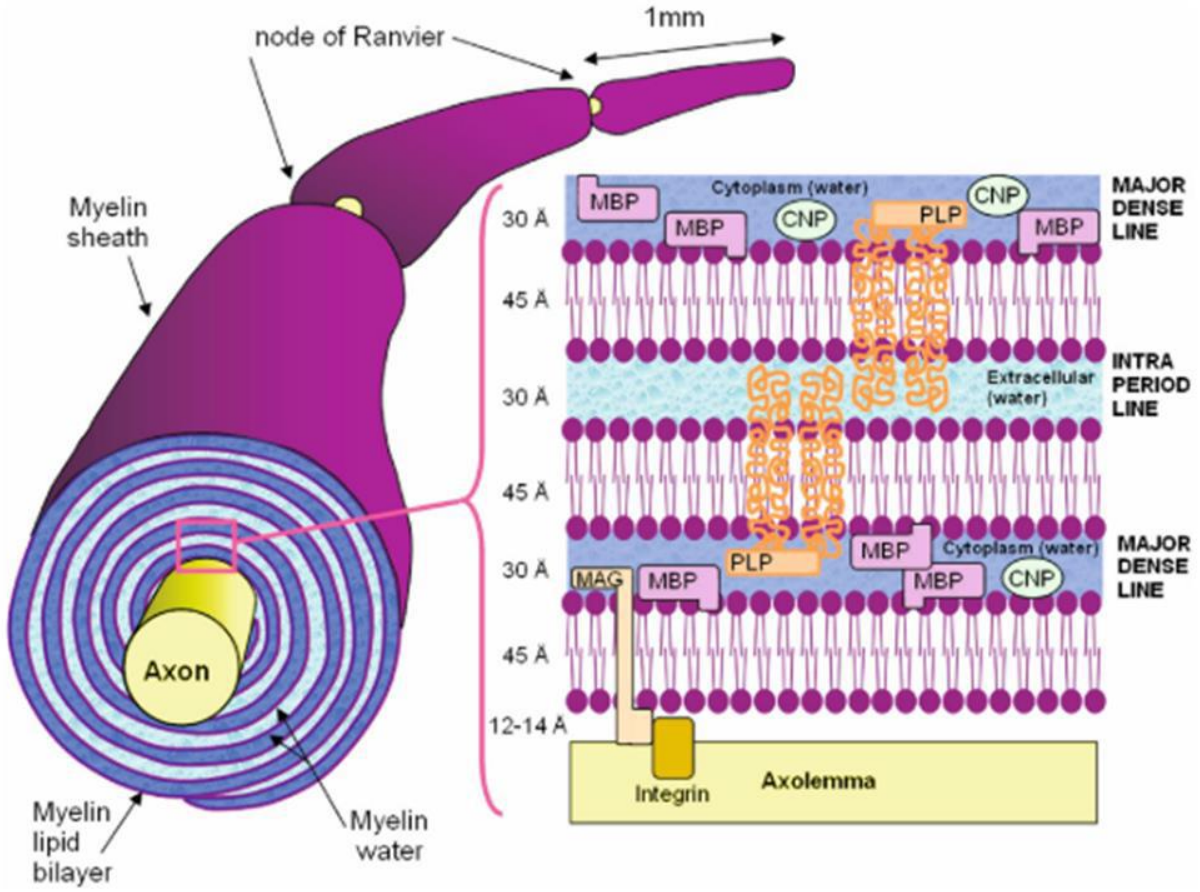


Figure 3: Structure of Myelin and its associated proteins. The position of CNP, PLP and MBP within the myelin layers and how they are associated with each other and the myelin membrane are shown (Laule *et al.*, 2007)

2. Aim and Objectives

The aim of this study is to investigate whether ibogaine administration induces remyelination of white matter in Sprague-Dawley rats.

Objective 1: To assess the effect of ibogaine administration on the expression of myelin-specific proteins and their genes: CNPase, MBP, and PLP, using quantitative immunoblotting and real time PCR.

Objective 2: To assess the effect of chronic morphine administration on CNPase, MBP, PLP mRNA and protein expression using real time PCR and quantitative immunoblotting.

Objective 3: To assess the effect of chronic morphine administration followed by ibogaine administration on CNPase, MBP, PLP protein and mRNA production using quantitative immunoblotting and real time PCR

Objective 4: To assess CNPase, MBP, PLP protein and mRNA expression 24 hours and 72 hours after ibogaine treatment to establish when remyelination begins.

3. Methods

3.1 Saline, Ibogaine and Chronic Morphine Administration to Sprague Dawley Rats

The animal ethics approval number obtained for this study was issued by the Animal Research Ethics Committee (2021/05/01/C) at the university of Witwatersrand. Fifty male Sprague-Dawley (SD) rats, post-natal days 42-45, were on a 12-hour light/dark cycle with food and water access as needed. All the animals were allowed a pre-treatment acclimatization period of one week. Two to three rats were housed in 1500U Techniplast Eurostandard Type IV S cages to prevent social isolation as it has been shown to impair remyelination in rats (Makinodan *et al.,* 2016). Animals were assigned randomly to one of five groups and weighed daily, to calculate accurate dosages of ibogaine, morphine and saline. The animals were randomly divided into 5 groups of 10 rats: saline control, ibogaine control, morphine control, a morphine ibogaine test group and a morphine ibogaine 2 test group with a 3-day waiting period before termination.

The saline control group (n=10) received subcutaneous (s.c.) saline (0.9% sodium chloride, Adcocare, Adcock Ingram Critical Care) ranging from 0.1 ml to 0.5 ml depending on the weight of the rat for 10 days and were sacrificed on day 11 (Figure 2). The ibogaine control group (n=10) received subcutaneous (s.c.) saline (0.9% sodium chloride, Adcocare, Adcock Ingram Critical Care) starting at 0.1ml and increasing to 0.5 ml over 10 days and a 50 mg/kg (Glick et al., 1991; Rezvani et al., 1995) intraperitoneal (i.p.) dose of ibogaine HCL (iboga Association, Cape Town) on day 11 and were sacrificed on day 12 (Figure 3). The ibogaine HCl was dissolved in saline (0.9% sodium chloride, Adcocare, Adcock Ingram Critical Care) using a homogenizer to create a homogenous and easily injectable liquid. The ibogaine has a 98% purity. The original morphine group (n=10) protocol was an escalated morphine regimen administered subcutaneously starting at 5 mg/kg morphine dosage on the 1st and 2nd day, 10 mg/kg on

the 3rd and 4th day and was increased by 5 mg/kg every second day until a 25 mg/kg dose was reached for day 9 and 10 (Blomqvist *et al.,* 2020)(Figure 2). These rats were sacrificed on day 11. This escalated morphine regimen has been shown to be effective in simulating opioid addiction in rats and avoiding morphine tolerance that can occur when giving the rats the same dose for 10 days. This regimen was unsuccessful as 6 out of 13 rats died before the regimen was completed, so the protocol was adjusted.

The new protocol used lower morphine doses over longer periods of time for the rats to adjust to the dosages. The new morphine regimen (n=7) administered subcutaneous morphine injections starting at 5 mg/kg for 2 days, 7,5 mg/kg for 3 days, 10 mg/kg for 3 days and 15 mg/kg for 2 days (Figure two). The rats were terminated on day 11. A maximum dose of 15 mg/kg was determined as most rats died after this dose in the previous protocol. Once morphine injections started the rats were moved from sawdust cages to paper cages to avoid suffocation which is further explained in appendix 2.1. The morphine-ibogaine group (n=10) received the adjusted escalated morphine regime for 10 days followed by a 50 mg/kg dose of ibogaine HCL on day 11. The rats were sacrificed on day 12. The second morphine-ibogaine group (n=10) received the same treatment as the first morphine-ibogaine group except the rats were terminated on day 15. The first morphine-ibogaine group allows us to evaluate remyelination directly after treatment and then the second morphine-ibogaine group is at the peak of remyelination which is 72 hours later (Skripuletz *et al.,* 2015). Rats were decapitated with a sharp, well-maintained guillotine on the day of termination.

3.1.1 White Matter Tissue collection from the Sprague Dawley Rat Brains

Brains were carefully removed from the skulls immediately following decapitation, the white matter regions were dissected from the brains on ice, transferred to separate 1.5 mL Eppendorf tubes and flash-frozen in liquid nitrogen prior to storage at -80°C for subsequent tissue processing.

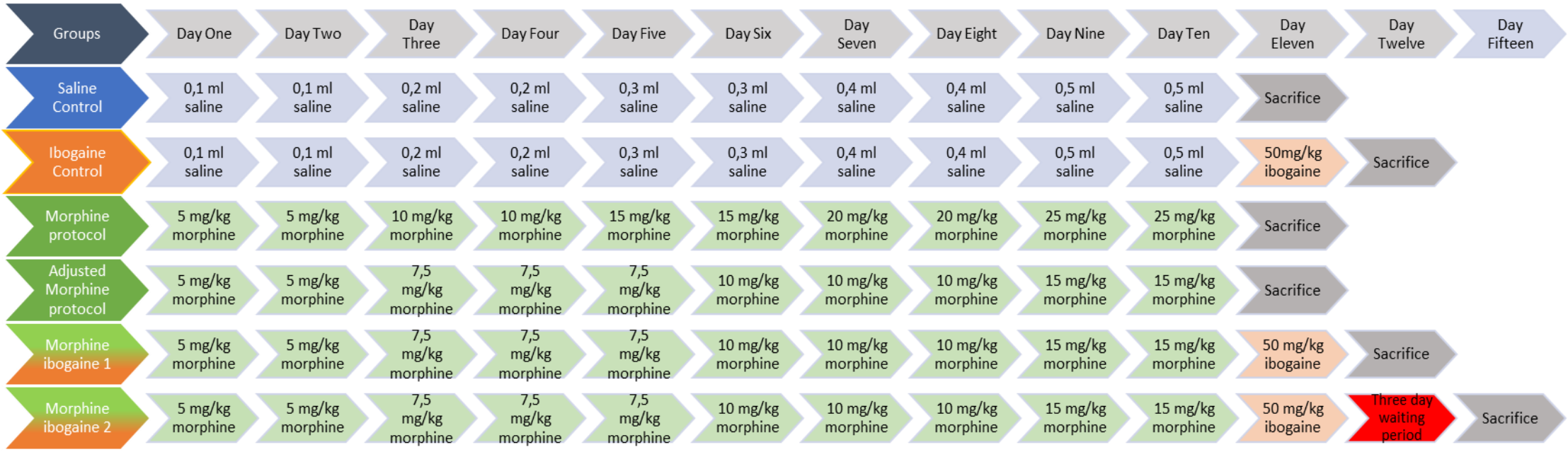


Figure 4: Morphine and Ibogaine Treatment Schedule for Sprague Dawley rats. The morphine and ibogaine treatments given to the (SD) rats. This is colour coded with saline doses in blue, morphine doses in green and ibogaine doses in orange. Dark grey is used for the day of termination.

3.2 White Matter Sample preparation for qPCR and Western Blotting

The frozen brain samples were homogenized with a homogenizer in QIAzol lysis reagent (Qiagen, Netherlands) to disrupt the cells. The QIAzol RNeasy Lipid Tissue Mini Kit (Qiagen, Netherlands) was used. This kit uses guanidine and phenol-based lysis with silica membrane purification. The guanidine thiocyanate and phenol allows for the lysis of lipid-based tissues and the inhibition of RNases. Manufacturer instructions were followed. The white matter tissue and lysis buffer homogenate was incubated on the benchtop for 5 minutes, 200 µl of chloroform was added and shaken for 15 seconds. The chloroform promotes separation of DNA, RNA and protein into phases. The homogenate was centrifuged for 15 minutes at 14500 rpm. The homogenate separated into three phases: RNA in the upper aqueous phase, DNA in the interphase and proteins in the lower organic phase.

The RNA was added to the silica membrane RNeasy column. The column, with the added RNA, was centrifuged for 15 seconds at 10000 rpm to allow the RNA to bind to the membrane and other contaminants could flow through. The column with the bound RNA was washed with a guanidine salt and ethanol buffer that removes nonspecific biomolecules such as carbohydrates, proteins or fatty acids. The column was also washed with a salt removing buffer (RPE buffer). RNase free water was added to the column and centrifuged for 1 minute at 10000 rpm to elute the RNA from the membrane. The collected RNA was stored at -80°C. The RNA was measured using the Thermo Scientific Nanodrop™ ND-1000 (Massachusetts, USA) to quantify and check the purity. This was done at 260 nm using 1 µl of total RNA.

The lower organic phase containing the proteins from the Qiazol lysis homogenate described previously was added to ice cold acetone in a 1:1 ratio left overnight in the freezer to precipitate the proteins from the Qiazol lysis mixture. The acetone-precipitate was centrifuged at 14500 rpm for 10 minutes and the supernatant was discarded. The pellet was airdried on ice in the Eppendorf tube for 10 minutes. This pellet was then homogenised with 5% sodium dodecyl sulphate (SDS). An alternative protein extraction method is described in appendix 2.2 as it was tested and produced much lower yields thus the acetone method was used. This acetone method was used as it yielded the most total protein as measured by BCA. Good protein yields were important as there is very little white matter tissue from the SD rat brains.

3.3 Bicinchoninic Acid (BCA) Assay of Total Proteins Extracted from White Matter

BCA assays are used to determine the concentration of total protein in a sample. This is done using a standard curve of Bovine Serum Albumin (BSA). BCA assays use protein in an alkaline solution or biuret solution to reduce Cu^{2+} into Cu^{1+} which is detected by bicinchoninic acid and produces a dark purple colorimetric measurement detected by the microplate reader. The protein samples that were prepared in 5% SDS were measured by diluting them with 5% SDS to 1:5, 1:10, or 1:20 depending on their concentration as the highest limit of this standard curve was 2000 µg/ml. The Pierce™ BCA Protein Assay kit (Thermoscientific, Massachusetts, USA) was used according to manufacturer instructions. Samples and the working reagent were added in duplicates to the plate in a 1:8 ratio of sample to working reagent. The plate was incubated at 37°C for 30 minutes and the absorbance read on the Biorad iMark™ microplate reader (Microplate Manager Software, Bio-Rad, USA) at 570nm.

3.4 Reverse Transcription of Extracted mRNA from white matter into cDNA

The Superscript™ III First Strand Synthesis system for RT-PCR (Invitrogen, Massachusetts, USA) was used to convert the RNA into cDNA. 2 µg of RNA was added to oligoDTs, water and dNTPs. The oligoDTs were used as they form more consistent small fragments of DNA than random hexamers. The oligoDTs bind to complementary polyA tails of mRNA so they start the transcription of the cDNA from the 3' end. This mixture was incubated at 65°C for 5 minutes and the on ice for a few minutes. The cDNA synthesis mix was made up of 1 µl of RNase OUT, 2 µl of 5X First-Strand buffer, 4 µl of 25 mM MgCl, 2 µl of 0,1 M DTT and 1 µl of Superscript III reverse transcriptase (200 U/µl). The RNA and cDNA synthesis mixtures were combined and incubated at 50°C for 50 minutes. The cDNA synthesis reaction was terminated at 85°C for 5 minutes this was done to ensure that mRNA stops transcribing cDNA as the enzyme is denatured. 1ul of RNase H was added and incubated at 37°C for 20 minutes. The RNase H degrades the template mRNA at the end of the process to ensure that only cDNA remains. The cDNA was measured using the spectrometer and diluted with RNase free water to 100 ng/µl. Aliquots were stored at 4°C.

3.5 Optimisation of Quantitative Polymerase Chain Reaction (qPCR) protocol for the cDNA from the White Matter of SD rats

Polymerase chain reaction is a technique to exponentially produce thousands of copies of DNA using specific primers, DNA polymerase and template cDNA. This is done by cycling through different temperatures to allow the polymerase to bind to the DNA and produce

multiple copies. The different temperatures are for the different processes of DNA replication to occur. These processes are denaturation which is done at 95°C to heat and separate the double stranded DNA, annealing where the primers bind to the single stranded DNA, the temperature for this process is determined by the primers' length and guanine-cytosine content. The last process is extension done by the DNA polymerase that extends the DNA from the 3' to 5' strands and this temperature is determined by the type of DNA polymerase.

The primers for MBP and CNP were run using a temperature gradient for the annealing step to determine the best temperature for each primer set. The primers used for the qPCRs are listed in table 2. This was done using PCR and agarose gels with ethidium bromide for visualisation from UV light exposure. The PCR reaction conditions were preincubation at 95°C for 10 minutes, 3 step amplification for 45 cycles with 95°C for 15 seconds, temperatures ranging from 70°C to 50°C for 20 seconds and 72°C for 30 seconds. The PCR products were then run on a 1% agarose gel at 100V with the Thermoscientific GeneRuler™ (Massachusetts, United States) which was then visualised using the ChemiDoc™ MP imaging system (Bio-Rad, Hercules, CA, USA). All primer sets worked efficiently at 51°C when tested on cDNA and plasmid DNA (Figure 5). Once the ideal annealing temperature was determined we continued with the qPCR protocol. An additional MBP primer set, designated MBP2, was also tested (Figure 5). This primer set was forward primer: 5'-CAA TGG ACC CGA CAG GAA AC-3' and reverse primer: 5'-TGG CAT CTC CAG CGT GTT C-3 (Jadasz et al., 2013). This primer set did not work (Figure 5).

Table 2:Primers for genes used in qPCR (CNP, MBP, PLP and beta actin)

Gene	**Forward Primer**	**Reverse Primer**
CNP (Hattori et al., 2014)	5'-CAA CAG GAT GTG GTG AGG A-3'	5'-CTG TCT TGG GTG TCA CAA AG-3'
MBP (Ray et al., 2003)	5'-TGA AAA CCC AGT AGT CCA C-3'	5'-GGA TTA AGA GAG GGT CTG C-3'
PLP (Ray et al., 2003)	5'-TAG GAC ATC CCG ACA AGT-3'	5'-AAA CAG GTG GAA GGT CAT T-3'
β-actin (Ray et al., 2003)	5'-TAC AAC CTC CTT GCA GCT CC-3'	5'-GGA TCT TCA TGA GGT AGT CTG TC-3'

The 10 µl qPCR reactions consisted of 2 µl of 2X Fast SYBR™ Green Master Mix (Thermofischer Scientific, Massachusetts, United States), 0.6 µl of combined reverse and forward primers (100 µm) (Inqaba Biotec™, Pretoria, South Africa), 1 µl of cDNA (100 ng per sample) and 6.4

µl of milliQ water. These reactions were set up in a Lightcycler® 96 well plates. Each sample was run in triplicate along with their beta actin housekeeping gene on the same plate. Each plate contained negative controls which contained no DNA just the mastermix, primers and water run in triplicate for the housekeeping gene and relevant gene of interest. The reactions were run on the Lightcycler® 96 (Roche Diagnostics, Indianapolis, United States of America). The thermal cycling conditions were as follows: preincubation at 95°C for 10 minutes, 3 step amplification for 45 cycles with 95°C for 15 seconds, 51°C for 20 seconds and 72°C for 30 seconds. This was ended with a melting curve to ensure that all the signals read were for the same product. The melting curve conditions were 95°C for 10 seconds, 65°C for 1 minute and 97°C for 1 second. Once this was done the LightCycler® 96 Software (Roche Diagnostics, Indianapolis, United States of America) was used to analyse the Cq values of the samples.

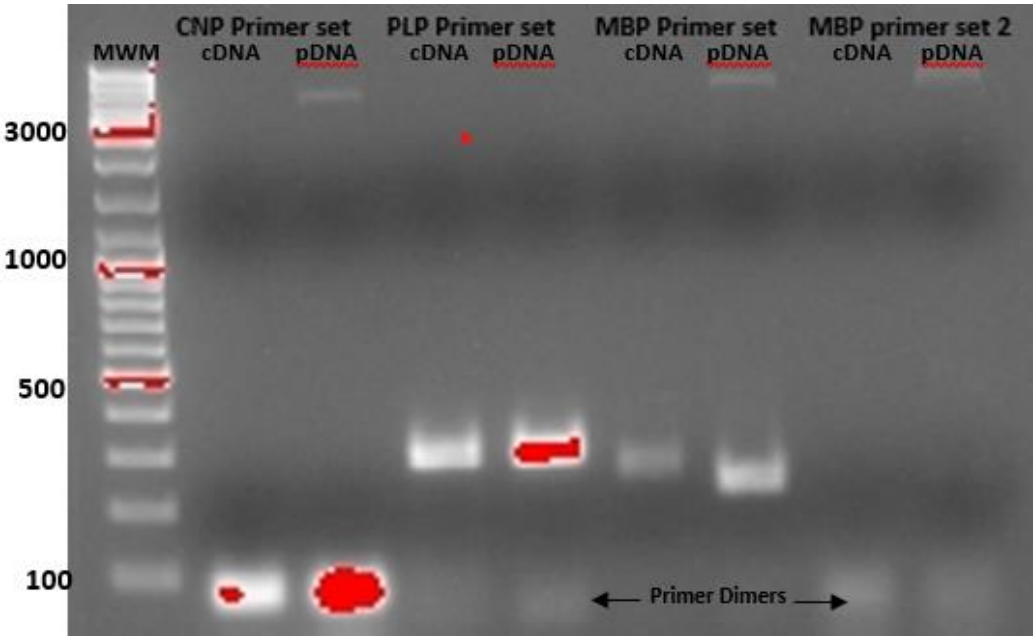


Figure 5: Agarose gel of CNP, PLP and MBP Primers tested at 51°C. The agarose gels showed positive bands for CNP, PLP and MBP primer sets. The CNP PCR product was approximately 100bp. The PLP PCR product was approximately 400bp. The MBP PCR product was approximately 400bp. The MBP PCR product was approximately 300bp.

3.5.1 The Pfaffl Method for analysis of qPCR data

The Pfaffl method uses the comparison of a target gene Cq value to its housekeeping genes' Cq while accounting for changes in efficiencies between multiple reaction plates. In our study we used the target genes: CNP, MBP and PLP and housekeeping gene: β-actin. The Pfaffl method was chosen as we had different efficiencies within the groups and genes of interest,

and it normalises the data against the housekeeping gene and saline control group. The delta delta Cq value was then used to determine the fold change per group using the efficiency.

$$\Delta\Delta Cq = (Cq_{\text{gene of interest}} - Cq_{\beta\text{-actin}})_{\text{test group}} - (Cq_{\text{gene of interest}} - Cq_{\beta\text{-actin}})_{\text{saline group}}$$

$$Fold\ change = E^{-\Delta\Delta Cq}$$

3.6 SDS PAGE of the White Matter Total Protein from SD Rats

Sodium dodecyl sulphate polyacrylamide gel electrophoresis uses electric current to move charged particles (like proteins) through the electric field towards the anode. The meshwork of the gel separates proteins based on size by allowing smaller proteins to pass through easily while larger proteins migrate slower. This technique was used to separate the proteins in the white matter tissue in gel to be transferred onto a nitrocellulose membrane during western blotting.

The samples were denatured and prepared for the SDS-PAGE. The samples were prepared by mixing them with reducing sample buffer and heating at 93°C for 5 minutes to denature the proteins. The reducing sample buffer contained 10% dodecyl sulphate sodium salt, an anionic detergent, to denature secondary and tertiary structures of protein and add a uniform negative charge to proteins linearising the protein. 10% β-mercarptoethanol in the buffer breaks disulphide bonds in the proteins therefore reducing the protein, and the presence of 20% glycerol creates a denser solution for the samples. Bromophenol blue was used as a tracking dye and Tris to buffer the solution at a pH of 6.8.

The SDS-PAGE gel was polymerized with a 4% stacking gel and 15% resolving gel. Acrylamide and N.N-methylenebisacrylamide form the meshwork of the gel after polymerization. 10% Ammonium persulfate was used as the initiator reagent and TEMED (N, N, N, N-tetramethyl ethylenediamine) (Sigma-Aldrich, Munich, Germany) was used as a catalyst for the polymerization. The stacking gel is more acidic (pH=6.8) in which glycine is a zwitterion ion allowing for it to become the trailing ion with chlorine being the leading ion, causing all proteins to stack between them before entering the resolving gel at the same time. The resolving gel is more basic and contains smaller pores. Here, the chloride and glycine ions move ahead of the proteins and proteins can now be separated according to their mass to charge ratio.

Each gel contained a lane of control protein to ensure consistency of results and eliminate inter-gel variability. The control protein is the same sample added to every gel. Equal volumes of sample were loaded and electrophoresed at 100V with a maximum current of 400 mA until the loading dye reached the bottom of the gel.

3.7 Western blotting and immunofluorescence of the White Matter Samples

The proteins from the SDS PAGE gel were transferred to a nitrocellulose membrane using a wet transfer system. The western blot transfers the proteins using electrophoresis to move the proteins from the gel onto the nitrocellulose membrane. A wet transfer system was chosen as the proteins are quite large and from mammalian tissue which can be harder to transfer using quicker methods such as a semi-dry system. The transfer was done at 35 V overnight at 4°C in the Hoefer™ T22 mighty small transfer tank (Massachusetts, United States). This yielded the best results as the gels retained almost no protein when stained with Coomassie post-transfer.

The nitrocellulose membranes were blocked for one hour using tris buffered saline (Trizma® hydrochloride, Sigma-Aldrich, Munich, Germany) with bovine serum albumin (Sigma-Aldrich, Munich, Germany) (TBS-BSA). The blocking is to ensure that there is no non-specific binding with the membrane and the antibodies which can cause background during imaging. The primary antibody incubation was done for an hour with the concentrations as follows: Anti-CNPase antibody (1:10000) (Abcam, Cambridge, United Kingdom), Anti-Myelin Basic Protein antibody (1:2000) (Biolegend, California, USA), Anti-Myelin PLP antibody (1:1000) (Abcam, Cambridge, United Kingdom), Anti-beta Actin antibody (1:2500) (Abcam, Cambridge, United Kingdom). The antibodies were diluted in TBS-BSA except beta actin which was in TBST-BSA (tris buffer saline with Tween-20). Beta actin needed to be diluted in TBST as there was dark background on the chemidoc images which shows non-specific binding of the primary antibody when the antibody was diluted in TBS. The membranes were washed 3 times for 10 minutes with TBST. The beta actin membranes used a TBST with a higher concentration of Tween-20 to reduce the background. The membranes were incubated for one hour at room temperature with the secondary goat anti-mouse HRP conjugated antibody. The concentrations for the Goat Anti-Mouse IgG H&L (HRP) (Abcam, Cambridge, United Kingdom) were as follows for the corresponding primary antibody: CNP, PLP and MBP (1:5000) and β-actin (1:2500). The membranes were washed two times for 10 minutes with TBST and a last

wash of 10 minutes with TBS to remove residual tween before imaging as the tween interferes with the chemiluminescence.

The membranes were incubated with the Pierce™ ECL Western Blotting Substrate (Thermofischer Scientific, Massachusetts, United States) for 5 minutes. The ECL substrate which contains luminol binds to the HRP on the secondary antibody which reacts to emit light which is then detected by the imaging system. The blots were imaged in the ChemiDoc™ MP imaging system (Bio-Rad, Hercules, CA, USA). These images were analysed for peak density using the QuantityOne™ version 4.6.9 Software Programme (Bio-Rad, Hercules, CA, USA). The data was then normalised using the following formula for all proteins:

$$Samples\ Protein\ expression = \frac{sample\ densitometric\ measurement\ /_{loading\ control\ from\ membrane}}{actin\ densitometric\ measurement\ /_{loading\ control\ of\ actin\ membrane}}$$

These protein expressions were averaged for each sample as they were run in duplicate. All the western blots that were analysed are included in the appendix section A3.

4. Statistical analysis

All statistical analysis was done using GraphPad Prism 9.5.0 for Windows (GraphPad Software, San Diego, California USA, www.graphpad.com). Shapiro-Wilk tests were run to test for normality. Unpaired t-tests and Mann-Whitney tests were run to determine significance between the groups to determine their significance dependent on the normality of the data. Outliers were determined at 1% using the ROUT method. The data is represented by mean±SD.

5. Results

All the western blots included in the results section are representative data as all the western blots analysed are included in the appendix section A3.

5.1 An immediate increase in mRNA fold expression of CNP after chronic morphine administration followed by ibogaine

Quantitative PCR was used to evaluate the changes in the mRNA expression of CNP in the white matter of SD rats after chronic morphine administration and ibogaine. Three outliers were found in this analysis: 1 in the morphine control, 1 in the ibogaine control and 1 in the morphine ibogaine 2 groups. These outliers were removed from the data set prior to analysis. The morphine ibogaine 1 group (4,856±6,034) showed a significant increase in the mRNA expression of CNP ($p=0,0010$) when compared to the saline control which equals 1 (Figure 6). This suggests that there are immediate increases in CNP gene expression following ibogaine administration after chronic morphine administration. The morphine control and ibogaine control showed no significant changes when compared to the saline control (Figure 6). This suggests that morphine and ibogaine alone has no effect on the fold expression of CNP. The morphine ibogaine groups show a significant increase ($p=0,0010$) in the morphine ibogaine 1 group but not the morphine ibogaine 2 group (1,734±1,530) (Figure 6). This suggests that ibogaine has an immediate effect on CNP mRNA expression and does not require a waiting period to change the expression of mRNA. The mRNA expression in morphine ibogaine 2 is not significantly greater than the saline control showing that, although there is an immediate increase in the 24 hours post-ibogaine administration, this effect decreases by day 3.

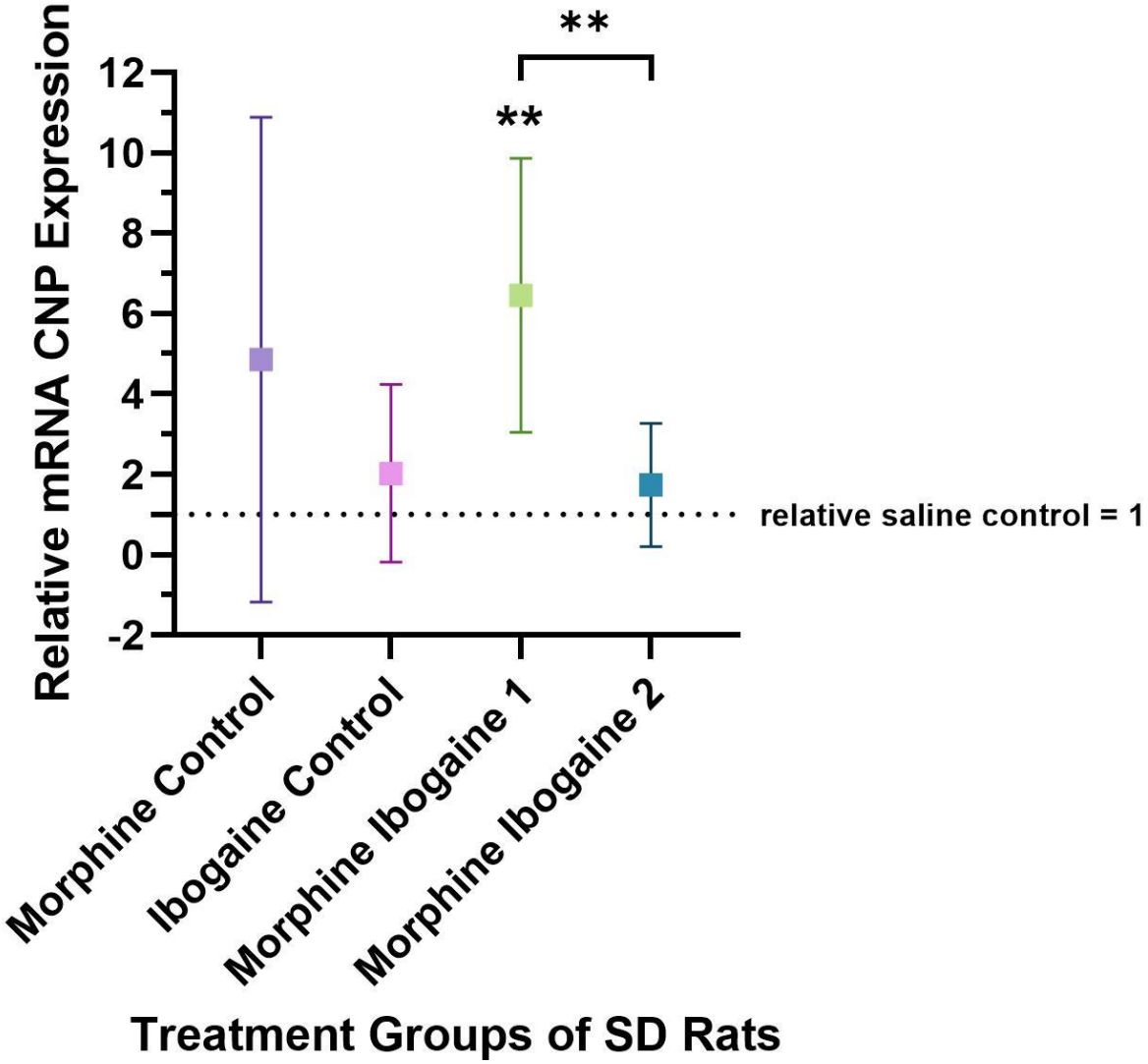
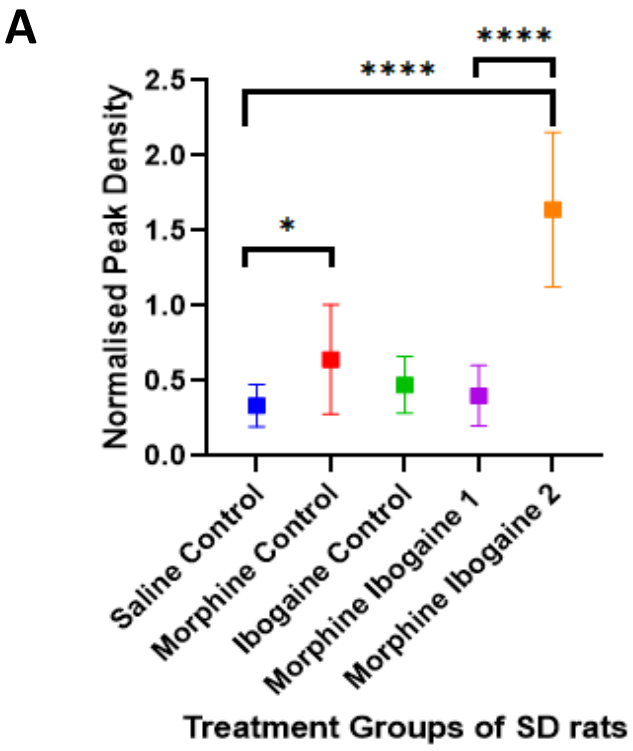


Figure 6: Relative expression of CNP gene shows an immediate increase in mRNA expression of CNP after ibogaine administration following chronic morphine administration. mRNA expression of CNP gene in morphine control (n=6), ibogaine control (n=8), morphine ibogaine 1 (n=8) and morphine ibogaine 2 (n=7). The data is presented as Mean ± SD. ** shows significance (p≥0,0021) which is compared to saline.

5.2 Ibogaine administration after chronic morphine regimen increases CNPase protein expression 3 days post-administration in Sprague Dawley Rats

Densitometric measurements of the western blots showed that the protein expression levels of CNPase in the white matter of SD rats were significantly increased in the morphine ibogaine 2 group (1,641±0,515) relative to the saline control group (0,336±0,1404) (Figure 7). This was a highly significant finding (p<0,0001). This implies that after chronic morphine administration ibogaine needs the 3-day wait period to see the changes in CNPase protein expression. The morphine control (0,643±0,3647) had significantly increased CNPase expression relative to the saline control (p=0.0456). There were no significant changes relative to the saline control in the ibogaine control and morphine ibogaine 1 groups. This implies that ibogaine alone has no effect on CNPase protein expression and there is no immediate change in CNPase expression following chronic morphine administration and a dose of ibogaine. Figure 7A shows there is a highly significant increase between the morphine ibogaine groups 1 (0,4019±0,2006) and 2 (p,0,0001). This implies that morphine may increase CNP protein and there is a waiting period before ibogaine affects the CNPase protein expression level.



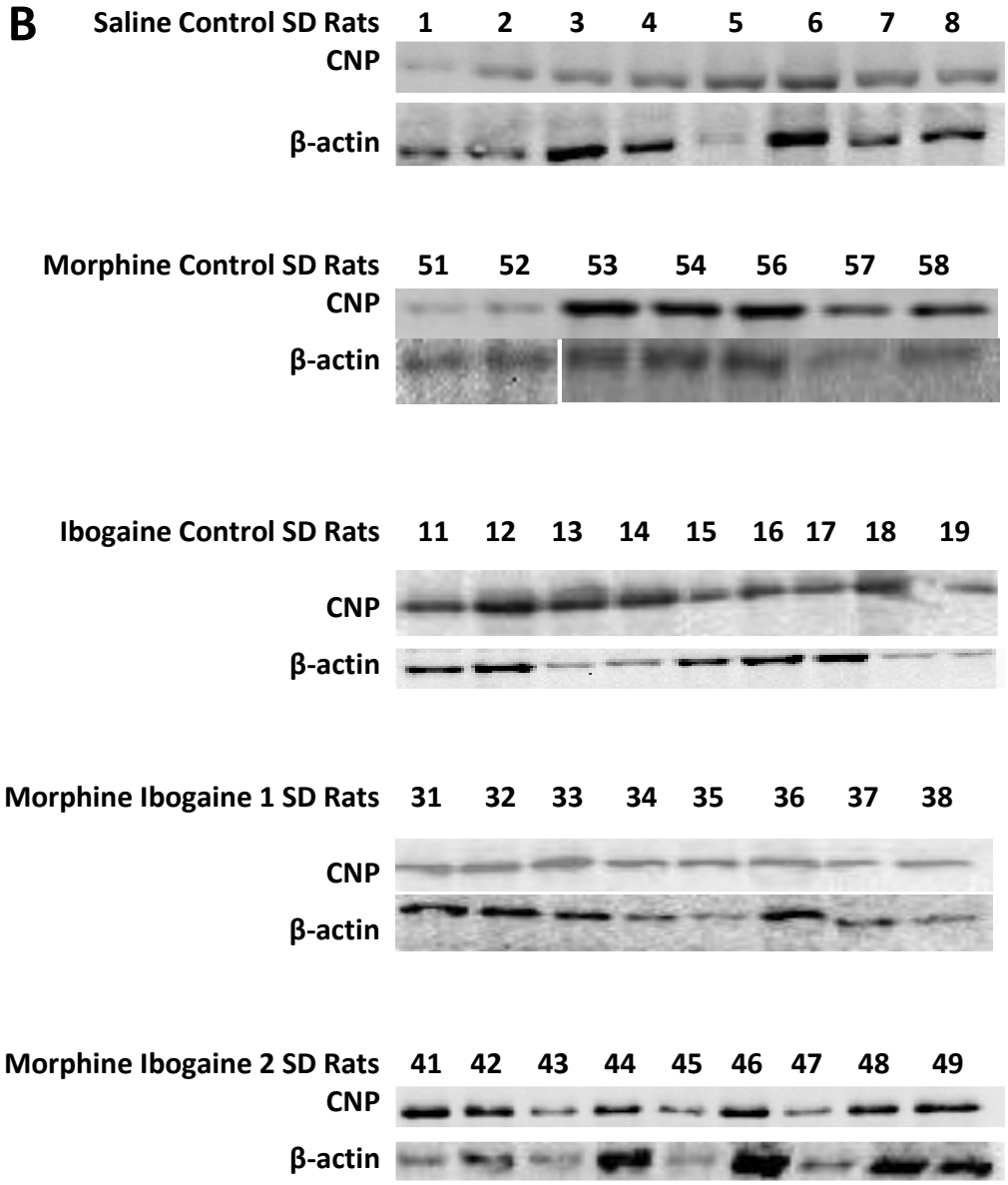


Figure 7: A-Peak density measurements and B- representative western blots of CNP protein expression of white matter in SD rats showed increased expression in morphine ibogaine treatment after a 3 day wait and in the morphine control group. Relative protein expression of CNP protein in saline control (n=8), morphine control (n=7), ibogaine control (n=9), morphine ibogaine 1 (n=8) and morphine-ibogaine 2 (n=9). The data is presented as mean ± SD. * shows significance ($p<0.05$) ** shows significance ($p<0.0001$).**

5.3 Ibogaine decreases MBP fold expression of mRNA in Sprague Dawley rats when administered alone

Quantitative PCR was used to evaluate the changes in the mRNA expression of MBP in the white matter of SD rats after chronic morphine administration followed by ibogaine administration. Two outliers were found in this analysis: 1 in the ibogaine control and 1 in the morphine ibogaine 2 groups. These outliers were removed from the data set prior to analysis. qPCR of the MBP gene shows highly significant decrease in fold expression ($p<0,0001$) in the ibogaine control group (0,2227±0,1740) compared to the saline control (Figure 8). This unexpected finding suggests that when ibogaine is administered alone it causes decreases in the gene expression of MBP. The morphine control group showed no significant changes when compared to the saline control (Figure 8). The morphine ibogaine 1 ($p=0,0381$) and morphine ibogaine 2 groups ($p=0,0411$) showed significant increases in MBP gene expression relative to the saline control (Figure 8). This suggests an immediate and prolonged increase in MBP mRNA expression following ibogaine administration after chronic morphine administration. It seems the prolonged effect is slightly larger than the saline control, albeit insignificantly so.

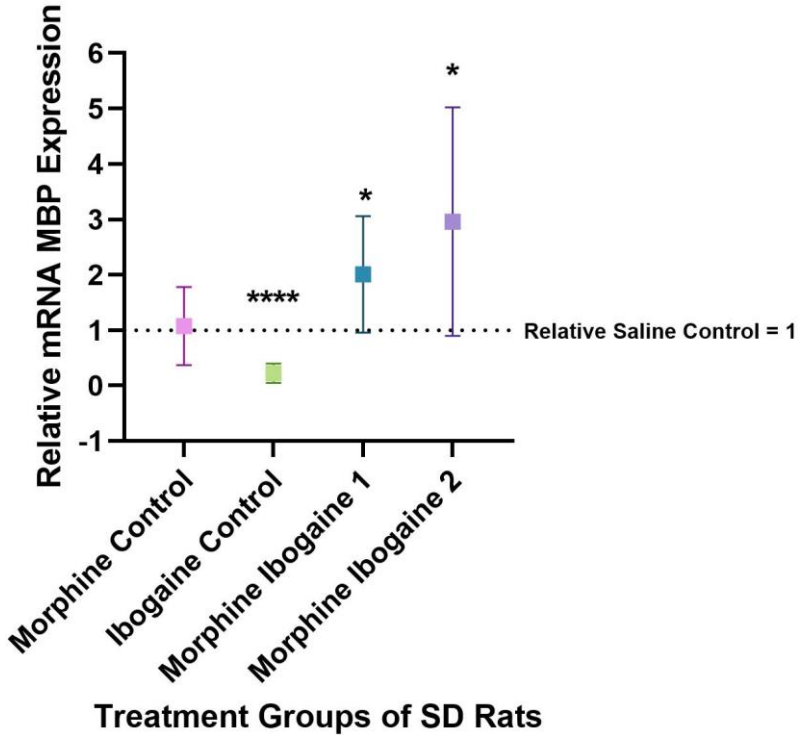


Figure 8: Relative mRNA expression of MBP is decreased after ibogaine administration. Relative mRNA expression of MBP gene in morphine control (n=7), ibogaine control (n=8), morphine ibogaine 1 (n=8) and morphine-ibogaine 2 (n=7). The data is presented as mean ± SD. *shows significance (p≥0,05) ** shows significance (p>0,0001). Increased fold expression is seen in both morphine ibogaine treatment groups.**

5.4 Increased MBP (18,5 kDa) protein expression after ibogaine administration

Western blots of the white matter from the SD rats showed a significant increase in the ibogaine control (1,204±0,5405) relative to the saline control group (Figure 9A). The morphine ibogaine 2 group (1,565±0,9011) showed a significant increase (p=0,0037) in protein expression of the 18.5 kDa isoform of MBP when compared to the saline control group (0,7271±0,2595) (Figure 9A). The morphine control and morphine ibogaine 1 groups showed no significant changes when compared to the saline control (Figure 9A). The morphine ibogaine 2 group is significantly increased when compared to the morphine ibogaine 1 group (0,5965±0,3139) suggesting that the MBP 18.5kDa isoform is increased after the three-day waiting period (p=0,0016). The MBP 21,5 kDa isoform shows no significant changes between groups (Figure 9B).

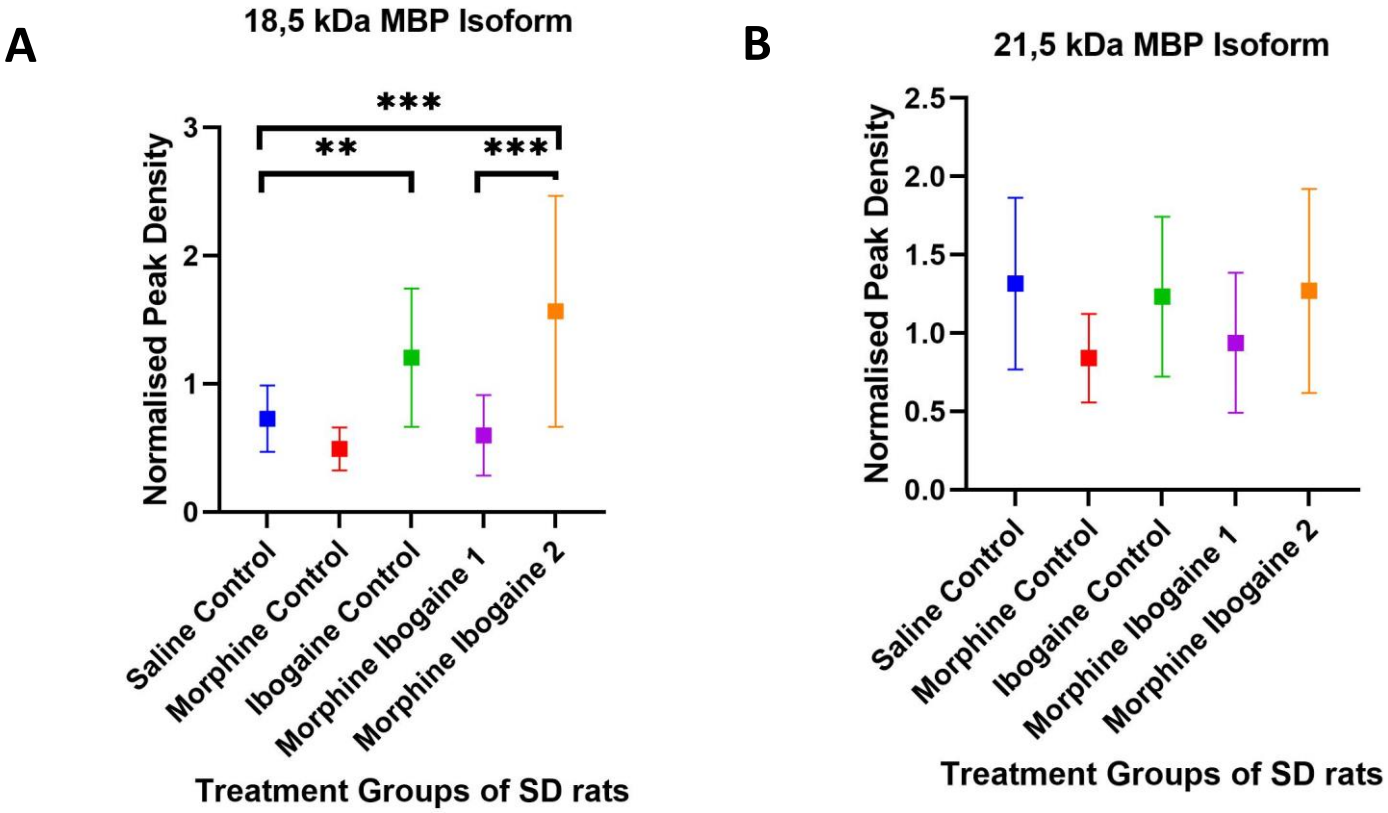


Figure 9: Peak density of MBP in white matter of the SD rats showed increased MBP expression after ibogaine administration. Graph 9A shows the peak density of the 18,5 kDa isoform. This shows the saline control (n=8), morphine control (n=6), ibogaine c control (n=9), morphine ibogaine 1 (n=8) and morphine-ibogaine 2 (n=9). ** shows significance (p≥0.0021) * shows significance (p≥0.0002). Graph 9B shows the peak density of the 21,5 kDa isoform which had no significance between groups.**

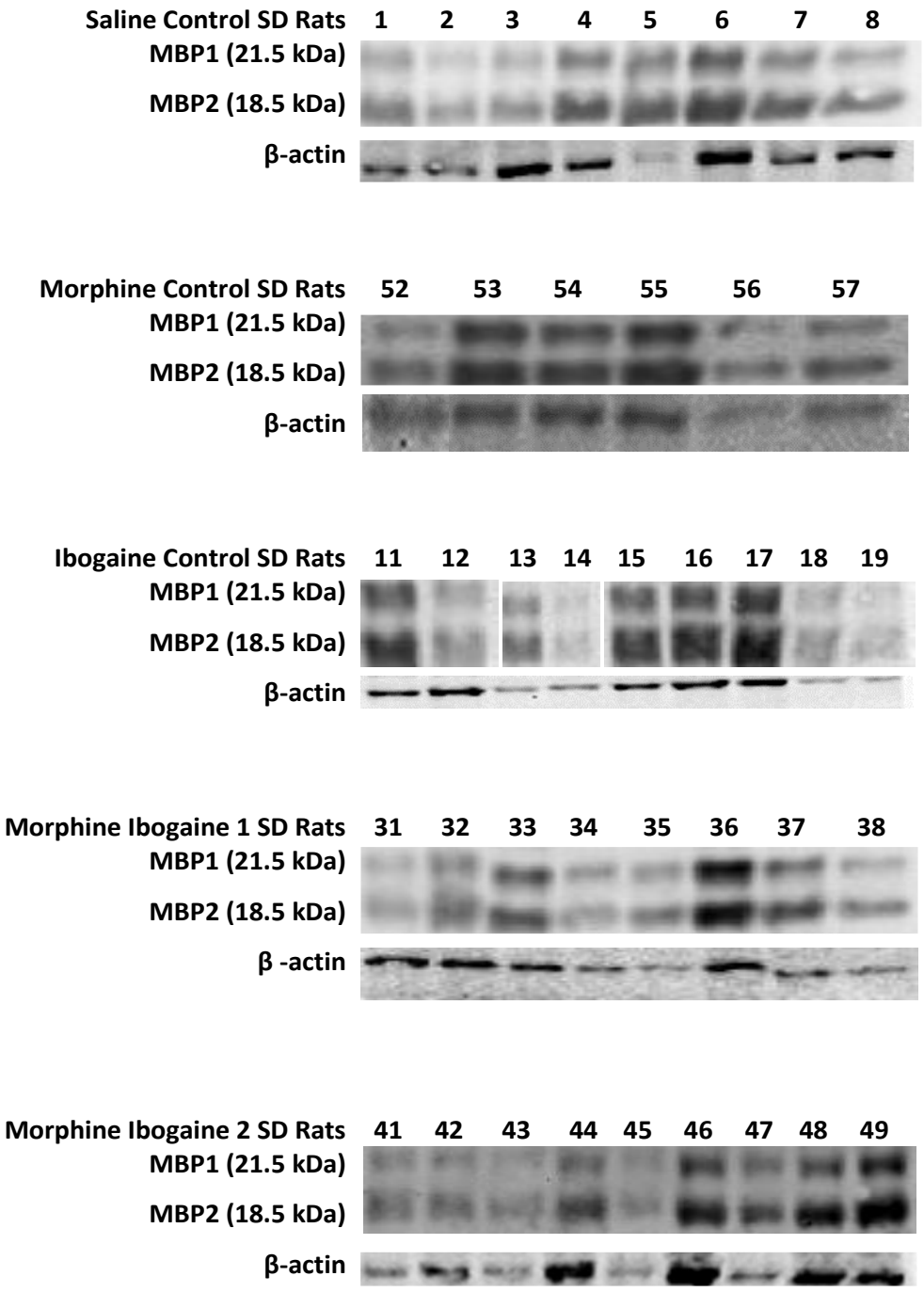


Figure 10: Representative western blots showing 21,5 kDa and 18,5 kDa isoforms of MBP. The immunoblots show the MBP probed samples with their corresponding β-actin probed samples.

5.5 Increased expression of PLP gene in ibogaine treated rats and decreased expression in chronic morphine rats with an increased protein expression of PLP in 3-day post ibogaine and chronic morphine treated rats

Quantitative PCR was used to evaluate the changes in the mRNA expression of PLP in the white matter of SD rats after chronic morphine administration and ibogaine. Three outliers were found in this analysis: 1 in the morphine control, 1 in morphine ibogaine and 1 in the morphine ibogaine 2 groups. These outliers were removed from the data set prior to analysis. The morphine control (0,2132±0,2027) showed significantly decreased PLP gene expression relative to saline control (p=0,0006). Significantly increased PLP expression is seen in the ibogaine control (5,043±4,367) when compared to the saline control (p=0,0003). In Figure 11 a significant decrease in PLP mRNA expression can be seen in the morphine ibogaine 2 group (0,3189±0,2777) relative to the saline control (p<0.0001). The morphine ibogaine 1 group showed no significant changes relative to saline control (Figure 11). These qPCR findings suggest that ibogaine has an increasing effect on PLP gene expression but does not have this effect when combined with chronic morphine. Morphine decreases PLP gene expression when used alone and in combination with ibogaine. The PLP protein expression shows an increase in morphine ibogaine 2 group when compared to morphine ibogaine. This suggests that the 3-day waiting period does influence PLP protein expression. This is the opposite of the qPCR results between the morphine ibogaine groups (Figure 11).

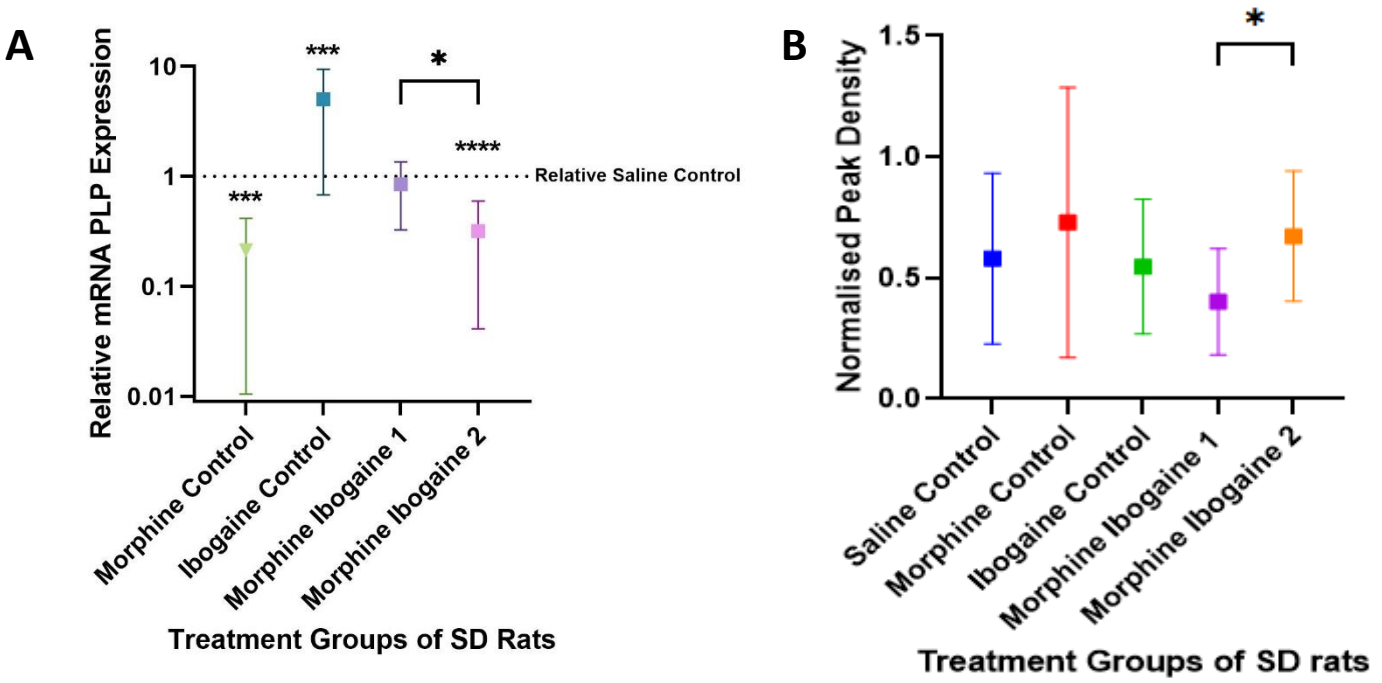


Figure 11: Relative Fold expression (9A) and peak density (9B) of PLP1 from qPCR and western blots of white matter of SD rats shows increase in morphine ibogaine groups. Relative mRNA expression of PLP1 gene in morphine control (n=7), ibogaine control (n=8),, morphine ibogaine 1 (n=7) and morphine-ibogaine 2(n=9). The data is presented as mean ± SD. All treatment groups were compared with the control group. ** shows significance (p≥0.0021) * shows significance (p≥0.0002) and **** (p<0,0001) peak density on the left graph of saline control(n=8), morphine control (n=7), ibogaine control (n=9) morphine ibogaine 1 (n=8) and morphine ibogaine 2 groups (n=9). * Shows significance of (p≤0,05).**

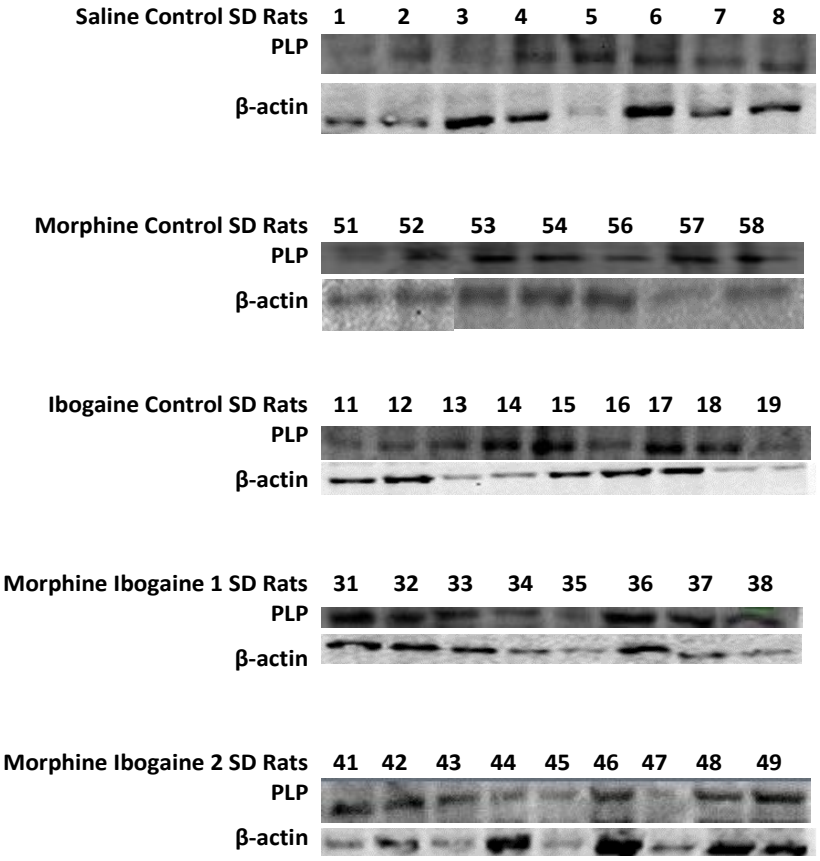


Figure 12: Representative western blots of the white matter from the SD rats probed for PLP. These immunoblots show the PLP probed samples with their corresponding β-actin probed sample

6. Discussion

The results showed that all myelin proteins had increased protein expression in the rats that were terminated 3 days after receiving the ibogaine dose when compared to the rats that were terminated 24 hours after receiving their ibogaine dose. This suggested that 72 hours or more is needed to see remyelination effects at a protein level. Morphine showed decreased PLP mRNA expression which is the only sign of demyelination in the study and suggests that a longer morphine regimen may be needed to induce demyelination at a detectable level. mRNA expression of PLP was the only myelin protein that reacted to the morphine and ibogaine controls in the way we expected as morphine decreased expression and ibogaine increased it. MBP had a decrease in mRNA expression from the ibogaine control which was unexpected. CNP showed increased protein expression in the morphine control which would need to be further investigated in the future.

Protein expression of CNPase was increased in the rats that were administered chronic morphine and rats that received chronic morphine followed by a dose of ibogaine with a 3 day wait prior to termination. This suggests the combination of morphine and ibogaine initially affects the mRNA expression which translates into increased CNPase protein expression between 24-72 hours. This finding is similar to what we found in our research from 2020 that showed increased CNPase protein following chronic morphine exposure (Govender *et al*., 2020). This is what leads us to believe that myelin is affected by morphine and ibogaine. There was decreased expression of the MBP gene in chronic morphine treated rats but increased gene expression in the combination treated chronic morphine and ibogaine groups. This suggests that the mRNA expression of MBP is affected immediately and sustained over the 3-day period. Morphine has an immediate decreasing effect on both PLP and MBP mRNA expression. MBP protein expression was increased in the ibogaine treated rats and in the combined chronic morphine and ibogaine treated rats. This suggests that ibogaine affects MBP with or without chronic morphine use. Ibogaine only treated rats showed increased PLP mRNA expression while there was a decrease in PLP mRNA expression in the rats treated with a combination morphine and ibogaine followed by a three day wait before termination. There is a common theme for all the myelin protein expression findings of the combination morphine and ibogaine groups, suggesting there is always increased expression in the rats terminated 3 days after receiving the ibogaine dose when compared to the rats terminated

24 hours after receiving their ibogaine dose. This suggests that the 3-day waiting period was necessary to evaluate the remyelination that could occur following chronic morphine administration and a single ibogaine dose.

Ibogaine has long term effects on substance addiction by reducing cravings. Its anti-addictive properties have since been used to assist in addiction therapy. The exact cause of these long-term effects are still largely unknown. This study suggests that this may be due to ibogaine inducing remyelination. Ibogaine administration alone increased myelin basic protein expression as the ibogaine control showed increased protein expression specifically in the 18,5 kDa isoform. This finding suggests that ibogaine may affect MBP protein expression although the mRNA fold expression of MBP was decreased in the ibogaine control group relative to the saline control.

The two isomers of myelin basic protein that were seen in the western blots were 21.5 kDa and 18.5 kDa. The 18.5 kDa was increased in the morphine-ibogaine 2 group (p=0,0037) as it is produced later in the remyelination process than the 21,5 kDa isoform (Harauz and Boggs, 2013). The 21.5 kDa isoform showed no significant changes in protein expression between the test groups. The morphine ibogaine 2 group has increased MBP expression when compared to the morphine ibogaine 1 group. This implies that the 3-day wait period between the two groups had a significant impact on the progress of remyelination.

The correlation between protein and mRNA expression is understudied with many conflicting results (Guo *et al.,* 2008). There seems to be an opposing relationship between the protein and mRNA expression. This is seen in CNP as the qPCR results showed an increase in mRNA expression in the morphine ibogaine 1 group (p=0,0010) relative to saline control but the protein expression of the morphine ibogaine 1 group did not change. In the combination morphine ibogaine groups the rats terminated after 24 hours have increased mRNA expression relative to saline but the opposite is seen for the protein expression as the morphine ibogaine 2 group is increased when compared to the morphine ibogaine 1 group. This trend is also seen with MBP where the gene expression is decreased for the ibogaine control, but the protein expression is increased. PLP shows similar findings as the morphine ibogaine 1 group has increased gene expression when compared to morphine ibogaine 2, but the protein expression shows an increase in the morphine ibogaine 2 group compared to

morphine ibogaine 1 group. This is an interesting trend as it is seen in all the myelin proteins where the mRNA expression is the opposite of the protein expression.

Transcription factors would play a major role in this relationship between the gene and protein expression. Sox2 has been identified as a crucial transcription factor for remyelination as it regulates OPC proliferation (Zhang *et al.,* 2018; Zhao *et al*., 2015). Sox2 regulates OPC proliferation by increasing proliferation of the OPCs and inhibits their differentiation into mature oligodendrocytes (Zhang *et al.,* 2018; Zhao *et al.,* 2015). This would be essential for remyelination to occur. The transcription factors Olig1 and Olig2 have also been linked to remyelination (Yang *et al.,* 2017). Olig1 assists in regulating myelin gene expression during remyelination and then the phosphorylated form assists with differentiation from OPCs into mature oligodendrocytes (Zhao *et al*., 2019). In adults, Olig2 can promote differentiation of OPCs into myelinating oligodendrocytes during remyelination of demyelinated areas (Wegener *et al.,* 2015; Yang *et al.,* 2017). Another major transcription factor that is required for efficient remyelination and oligodendrocyte regeneration is Stat3 (Steelman *et al*., 2016). Stat3 is an essential transcription factor and when increased it facilitates OPC differentiation and remyelination following injury (Steelman *et al.,* 2016). The effects of these transcription factors on OPCs show promising pathways for increasing remyelination and making it more efficient. These factors should be investigated under the influence of ibogaine to understand if they are possible mechanisms of action for the psychedelic.

Brain derived neurotrophic factor (BDNF) has been shown to increase the expression of MBP and PLP in oligodendrocytes (Du *et al*., 2006b, 2006a; Xiao *et al.,* 2009). This could be the direct influence that ibogaine has on MBP protein expression, as ibogaine administration increases the expression of BDNF in the brain (Marton *et al.,* 2019). This increase may only be seen in MBP as PLP is produced later in the remyelination process as it follows the same a pattern of reappearance as developmental myelination (Baumann and Pham-Dinh, 2001; Gudi *et al.,* 2009; Maier *et al.,* 2008). The process of remyelination requires the use of adult oligodendrocyte progenitor cells to undergo development and form new mature oligodendrocytes to remyelinate the axons after demyelination has occurred. These progenitor cells undergo 3 phases: activation to change their shape and gene expression at the site of demyelination, proliferation and migration to increase the number of cells available in the demyelinated area and finally differentiation into mature oligodendrocytes to form the

myelin around the demyelinated axon (Barateiro and Fernandes, 2014; Uyeda and Muramatsu, 2020). CNP and MBP are the earliest markers of remyelination from the myelin proteins usually detected after 3-4 days (Skripuletz *et al.,* 2011). This explains the increase in protein expression of CNP ($p<0.0001$) and MBP (18.5 kDa) ($p=0,0037$) only seen in the morphine ibogaine 2 group and no increases in protein expression seen in morphine-ibogaine 1.

Demyelination by opioids has been researched using MRIs in humans. Opioid addiction has shown decreased white matter integrity with decreases in radial diffusion which indicates myelin pathology (Bora *et al.,* 2012). Bora *et al*. also showed that longer drug use correlated with increased white matter injury. This suggests that the decreased myelin at a protein level could be undetectable as it appears in small quantities, and an extended time of morphine administration might be needed to see the major changes at a protein level. Li *et al*. (2013) found demyelination occurred in chronic heroin users, which supports that morphine decreases myelin (Fan *et al.,* 2018). Our study would need to increase the length of chronic morphine administration to see a significant decrease in the myelin proteins. There is evidence that morphine decreases the gene expression of PLP ($p=0,0006$) compared to the saline control. This is not seen in the gene expression of the other myelin proteins.

Ibogaine is a kappa opioid agonist (Alper, 2001; Glick *et al.,* 1997; Glick and Maisonneuve, 1998). The kappa opioid receptor has been shown to influence remyelination through oligodendrocytes (Du *et al.,* 2016; Mei *et al.,* 2016). The kappa opioid receptor is an important regulator of oligodendrocyte differentiation and remyelination. This regulation is done by controlling the OPCs developing into oligodendrocytes (Du *et al.,* 2016; Mei *et al.,* 2016). The kappa opioid receptor is expressed on OPCs and in white matter such as the corpus callosum (Mei *et al*., 2016). This shows potential for ibogaine to be used through this receptor for long term remyelination as its metabolite noribogaine which has a long life within humans and is also a kappa opioid receptor agonist (Maillet *et al*., 2015). This possible route of action from ibogaine to cause remyelination is something we should explore. This could be used not just in abuse studies but also demyelinating diseases such as multiple sclerosis.

A limitation to the study was the unsuccessful qPCR standard curve which could be due to the low amounts of expression in the samples as we had to dilute the standard curve to

femtograms per microliter for the samples to fit within the curve. Once the samples fit the curve it showed high levels of variability among the concentrations measured even though the R-values were within 90-98% and the Cq values were close together. The escalated morphine regimen used very low doses due to rats dying at higher doses, in future studies we should use a longer regimen of a few weeks to increase the chances of seeing an actual change in the myelin proteins such as in the cuprizone model of demyelination which is over 5 weeks. Another limitation is the absence of an ibogaine treated group that had a 72-hour withdrawal which would allow us to better evaluate the effects of ibogaine alone on myelination.

Future research directions could include the addition of a cuprizone group to stimulate known demyelination and treat with ibogaine over a longer period to see how much remyelination can occur. Immunohistochemistry of the white matter would allow us to observe the structural changes and the distribution of the myelin proteins after remyelination (M Lindner et al., 2008; Ludwin and Sternberger, 1984). A suggestion would be to investigate the mTOR gene protein in relation to ibogaine and myelination as psychedelics have been shown to increase mTOR expression (Ly *et al.,* 2018). mTOR is essential for oligodendrocyte differentiation and regulates CNP, MBP and PLP gene expression. This could be a possible mechanism of action of ibogaine inducing remyelination.

This study opens a new topic of discussion with ibogaine being able to remodel the brain and act as a psychoplastogen (Ly *et al.,* 2018). The secretion of neurotrophic growth factors and neural plasticity has been shown to occur following psychedelic treatment (Chi and Gold, 2020; Ly *et al.,* 2018; Marton *et al.,* 2019). This makes the compound more relevant to medicine outside of SUDs. The mechanisms of action for all these effects of ibogaine need further research to uncover its potential effects for pain management, opioid addiction and demyelinating disorders.

References

Akiyama, K., Ichinose, S., Omori, A., Sakurai, Y., Asou, H., 2002. Study of expression of myelin basic proteins (MBPs) in developing rat brain using a novel antibody reacting with four major isoforms of MBP. J Neurosci Res 68, 19–28. https://doi.org/10.1002/jnr.10188

Aleksandrova, L.R., Phillips, A.G., 2021. Neuroplasticity as a convergent mechanism of ketamine and classical psychedelics. Trends Pharmacol Sci 42, 929–942. https://doi.org/10.1016/j.tips.2021.08.003

Alper, K.R., 2001. IBOGAINE: A REVIEW, in: The Alkaloids. pp. 1–37.

Barateiro, A., Fernandes, A., 2014. Temporal oligodendrocyte lineage progression: In vitro models of proliferation, differentiation and myelination. Biochim Biophys Acta Mol Cell Res. https://doi.org/10.1016/j.bbamcr.2014.04.018

Barsuglia, J., Polanco, M., Palmer, R., Malcom, B., Kelmendi, B., Calvey, T., 2018a. Psychedelic Neuroscience. Psychedelic Neuroscience 424, 121–146.

Barsuglia, J., Polanco, M., Palmer, R., Malcom, B., Kelmendi, B., Calvey, T., 2018b. Psychedelic Neuroscience. Psychedelic Neuroscience 424, 121–146.

Barsuglia, J., Polanco, M., Palmer, R., Malcom, B., Kelmendi, B., Calvey, T., Howells, F., Corkery, J.M., 2018c. Psychedelic Neuroscience, Psychedelic Neuroscience. Acaddemic Press .

Baumann, N., Pham-Dinh, D., 2001. Biology of oligodendrocyte and myelin in the mammalian central nervous system. Physiol Rev 81, 871–927. https://doi.org/10.1152/physrev.2001.81.2.871

Belouin, S.J., Henningfield, J.E., 2018. Psychedelics: Where we are now, why we got here, what we must do. Neuropharmacology 142, 7–19. https://doi.org/10.1016/j.neuropharm.2018.02.018

Bogenschutz, M.P., Podrebarac, S.K., Duane, J.H., Amegadzie, S.S., Malone, T.C., Owens, L.T., Ross, S., Mennenga, S.E., 2018. Clinical interpretations of patient experience in a trial of psilocybin-assisted psychotherapy for alcohol use disorder. Front Pharmacol 9, 1–7. https://doi.org/10.3389/fphar.2018.00100

Boggs, J.M., 2006. Myelin basic protein: A multifunctional protein. Cellular and Molecular Life Sciences 63, 1945–1961. https://doi.org/10.1007/s00018-006-6094-7

Bonci, A., Williams, J.T., 1997. Increased probability of GABA release during withdrawal from morphine. Journal of Neuroscience 17, 796–803. https://doi.org/10.1523/jneurosci.17-02-00796.1997

Bora, E., Yücel, M., Fornito, A., Pantelis, C., Harrison, B.J., Cocchi, L., Pell, G., Lubman, D.I., 2012. White matter microstructure in opiate addiction. Addiction Biology 17, 141–148. https://doi.org/10.1111/j.1369-1600.2010.00266.x

Bouso, J.C., Fornís, I., Vilamala, M.V., De Loenen, B., Sainz-Cort, A., Jiménez-Garrido, D.F., Dos Santos, R.G., Hallak, J.E.C., Alcázar-Córcoles, M.Á., Jenks, C.W., 2020. An analytical study of iboga alkaloids contained in Tabernanthe iboga-derived products offered by ibogaine treatment providers. Rev Psiquiatr Clín 47, 51–54. https://doi.org/10.1590/0101-60830000000231

Brown, T.K., Alper, K., 2018. Treatment of opioid use disorder with ibogaine: detoxification and drug use outcomes. American Journal of Drug and Alcohol Abuse 44, 24–36. https://doi.org/10.1080/00952990.2017.1320802

Calleja-Conde, J., Morales-García, J.A., Echeverry-Alzate, V., Bühler, K.M., Giné, E., López-Moreno, J.A., 2022. Classic psychedelics and alcohol use disorders: A systematic review of human and animal studies. Addiction Biology 27, 1–13. https://doi.org/10.1111/adb.13229

Calvey, T., Howells, F., 2018. Psychedelic Neuroscience. Acaddemic Press .

Capello, E., Voskuhl, R.R., McFarland, H.F., Raine, C.S., 1997. Multiple sclerosis: Re-expression of a developmental gene in chronic lesions correlates with remyelination. Ann Neurol 41, 797–805. https://doi.org/10.1002/ana.410410616

Carnicella, S., Ron, D., 2009. GDNF - A potential target to treat addiction. Pharmacol Ther. https://doi.org/10.1016/j.pharmthera.2008.12.001

Cavaliere, F., Urra, O., Alberdi, E., Matute, C., 2012. Oligodendrocyte differentiation from adult multipotent stem cells is modulated by glutamate. Cell Death Dis 3, e268–e268. https://doi.org/10.1038/cddis.2011.144

Célèrier, E., Laulin, J.P., Corcuff, J.B., Le Moal, M., Simonnet, G., 2001. Progressive enhancement of delayed hyperalgesia induced by repeated heroin administration: A sensitization process. Journal of Neuroscience 21, 4074–4080. https://doi.org/10.1523/jneurosci.21-11-04074.2001

Chetty, Y.Y., Naidoo, P., Nadar, A., 2020. Tracing My Roots: An Ethnographic Review of "Sugars" Addiction. Oriental Anthropologist 20, 125–134. https://doi.org/10.1177/0972558X20913958

Chi, T., Gold, J.A., 2020. A review of emerging therapeutic potential of psychedelic drugs in the treatment of psychiatric illnesses. J Neurol Sci. https://doi.org/10.1016/j.jns.2020.116715

Cichewicz, D.L., 2004. Synergistic interactions between cannabinoid and opioid analgesics. Life Sci 74, 1317–1324. https://doi.org/10.1016/j.lfs.2003.09.038

Cichewicz, D.L., Haller, V.L., Welch, S.P., 2001. Changes in opioid and cannabinoid receptor protein following short-term combination treatment with Δ9-tetrahydrocannabinol and morphine. Journal of Pharmacology and Experimental Therapeutics 297, 121–127.

Compton, P., Charuvastra, V.C., Ling, W., 2001. Pain intolerance in opioid-maintained former opiate addicts: Effect of long-acting maintenance agent. Drug Alcohol Depend 63, 139–146. https://doi.org/10.1016/S0376-8716(00)00200-3

Crocq, M.-A., 2007a. Historical and cultural aspects of man's relationship with addictive drugs. Dialogues Clin Neurosci 9, 355–61. https://doi.org/10.31887/DCNS.2007.9.4/macrocq

Crocq, M.-A., 2007b. Historical and cultural aspects of man's relationship with addictive drugs. Dialogues in clinical neuroscience 9, 355–61. https://doi.org/10.31887/DCNS.2007.9.4/macrocq

Curtis, K., Viswanath, H., Velasquez, K.M., Molfese, D.L., Harding, M.J., Aramayo, E., Baldwin, P.R., Ambrosi, E., Madan, A., Patriquin, M., Frueh, B.C., Fowler, J.C., Kosten, T.R., Nielsen, D.A., Salas, R., 2017. Increased habenular connectivity in opioid users is associated with an α5 subunit nicotinic receptor genetic variant. American Journal on Addictions 26, 751–759. https://doi.org/10.1111/ajad.12607

Das, S., Barnwal, P., Ramasamy, A., Sen, S., Mondal, S., 2016. Lysergic acid diethylamide: a drug of 'use'? Ther Adv Psychopharmacol 6, 214–228. https://doi.org/10.1177/2045125316640440

De Gregorio, D., Enns, J.P., Nuñez, N.A., Posa, L., Gobbi, G., 2018. D-Lysergic acid diethylamide, psilocybin, and other classic hallucinogens: Mechanism of action and potential therapeutic applications in mood disorders, in: Progress in Brain Research. pp. 69–96. https://doi.org/10.1016/bs.pbr.2018.07.008

de Vos, C.M.H., Mason, N.L., Kuypers, K.P.C., 2021. Psychedelics and Neuroplasticity: A Systematic Review Unraveling the Biological Underpinnings of Psychedelics. Front Psychiatry 12. https://doi.org/10.3389/fpsyt.2021.724606

De Vries, H., De Jonge, J.C., Schrage, C., Van Der Haar, M.E., Hoekstra, D., 1997. Differential and cell development-dependent localization of myelin mRNAs in oligodendrocytes. J Neurosci Res 47, 479–488. https://doi.org/10.1002/(SICI)1097-4547(19970301)47:5<479::AID-JNR3>3.0.CO;2-E

Diana, M., 2011. The dopamine hypothesis of drug addiction and its potential therapeutic value. Front Psychiatry 2, 1–7. https://doi.org/10.3389/fpsyt.2011.00064

Du, C., Duan, Y., Wei, W., Cai, Y., Chai, H., Lv, J., Du, X., Zhu, J., Xie, X., 2016. Kappa opioid receptor activation alleviates experimental autoimmune encephalomyelitis and promotes oligodendrocyte-mediated remyelination. Nat Commun 7. https://doi.org/10.1038/ncomms11120

Du, Y., Fischer, T.Z., Clinton-Luke, P., Lercher, L.D., Dreyfus, C.F., 2006a. Distinct effects of p75 in mediating actions of neurotrophins on basal forebrain oligodendrocytes. Molecular and Cellular Neuroscience 31, 366–375. https://doi.org/10.1016/j.mcn.2005.11.001

Du, Y., Lercher, L.D., Zhou, R., Dreyfus, C.F., 2006b. Mitogen-activated protein kinase pathway mediates effects of brain-derived neurotrophic factor on differentiation of basal forebrain oligodendrocytes. J Neurosci Res 84, 1692–1702. https://doi.org/10.1002/jnr.21080

Eidson, L.N., Inoue, K., Young, L.J., Tansey, M.G., Murphy, A.Z., 2017. Toll-like Receptor 4 Mediates Morphine-Induced Neuroinflammation and Tolerance via Soluble Tumor Necrosis Factor Signaling. Neuropsychopharmacology 42, 661–670. https://doi.org/10.1038/npp.2016.131

Eidson, L.N., Murphy, A.Z., 2013. Blockade of toll-like receptor 4 attenuates morphine tolerance and facilitates the pain relieving properties of morphine. Journal of Neuroscience 33, 15952–15963. https://doi.org/10.1523/JNEUROSCI.1609-13.2013

Everitt, B.J., Wolf, M.E., 2002. Psychomotor Stimulant Addiction: A Neural Systems Perspective. Journal of Neuroscience 22, 3312–3320. https://doi.org/10.1523/jneurosci.22-09-03312.2002

Fan, W., Wang, H., Zhang, Y., Loh, H.H., Law, P.Y., Xu, C., 2018. Morphine regulates adult neurogenesis and contextual memory extinction via the PKCε/Prox1 pathway. Neuropharmacology 141, 126–138. https://doi.org/10.1016/j.neuropharm.2018.08.031

Fünfschilling, U., Supplie, L.M., Mahad, D., Boretius, S., Saab, A.S., Edgar, J., Brinkmann, B.G., Kassmann, C.M., Tzvetanova, I.D., Möbius, W., Diaz, F., Meijer, D., Suter, U., Hamprecht, B., Sereda, M.W., Moraes, C.T., Frahm, J., Goebbels, S., Nave, K.A., 2012. Glycolytic oligodendrocytes maintain myelin and long-term axonal integrity. Nature 485, 517–521. https://doi.org/10.1038/nature11007

George, D.T., Ameli, R., Koob, G.F., 2019. Periaqueductal Gray Sheds Light on Dark Areas of Psychopathology. Trends Neurosci. https://doi.org/10.1016/j.tins.2019.03.004

Glick, S.D., Maisonneuve, I.M., 1998. Mechanisms of antiaddictive actions of ibogaine, in: Annals of the New York Academy of Sciences. pp. 214–226. https://doi.org/10.1111/j.1749-6632.1998.tb08237.x

Glick, S.D., Maisonneuve, I.M., Pearl, S.M., 1997. Evidence for roles of κ-opioid and NMDA receptors in the mechanism of action of ibogaine. Brain Res 749, 340–343. https://doi.org/10.1016/S0006-8993(96)01414-X

Glick, S.D., Maisonneuve, I.M., Szumlinski, K.K., 2001. Mechanisms of action of ibogaine: Relevance to putative therapeutic effects and development of a safer iboga alkaloid congener. Alkaloids: Chemistry and Biology. https://doi.org/10.1016/S0099-9598(01)56006-X

Glick, S.D., Rossman, K., Steindorf, S., Maisonneuve, I.M., Carlson, J.N., 1991. Effects and aftereffects of ibogaine on morphine self-administration in rats. Eur J Pharmacol 195, 341–345. https://doi.org/10.1016/0014-2999(91)90474-5

Govender, D., Meulenberg, N., Owen, G., Calvey, T., 2020. Effects of Ibogaine on CNPase in the White Matter Tissue of Rats.

Gudi, V., Moharregh-Khiabani, D., Skripuletz, T., Koutsoudaki, P.N., Kotsiari, A., Skuljec, J., Trebst, C., Stangel, M., 2009. Regional differences between grey and white matter in cuprizone induced demyelination. Brain Res 1283, 127–138. https://doi.org/10.1016/j.brainres.2009.06.005

Guo, Y., Xiao, P., Lei, S., Deng, F., Xiao, G.G., Liu, Y., Chen, X., Li, L., Wu, S., Chen, Y., Jiang, H., Tan, L., Xie, J., Zhu, X., Liang, S., Deng, H., 2008. How is mRNA expression predictive for protein expression? A correlation study on human circulating monocytes. Acta Biochim Biophys Sin (Shanghai) 40, 426–436. https://doi.org/10.1111/j.1745-7270.2008.00418.x

Harauz, G., Boggs, J.M., 2013. Myelin management by the 18.5-kDa and 21.5-kDa classic myelin basic protein isoforms. J Neurochem. https://doi.org/10.1111/jnc.12195

Harker, N., Lucas, W.C., Laubscher, R., Dada, S., Myers, B., Parry, C.D., 2020. Is South Africa being spared the global opioid crisis? A review of trends in drug treatment demand for heroin, nyaope and codeine-related medicines in South Africa (2012–2017). International Journal of Drug Policy 83. https://doi.org/10.1016/j.drugpo.2020.102839

Hattori, T., Shimizu, S., Koyama, Y., Emoto, H., Matsumoto, Y., Kumamoto, N., Yamada, K., Takamura, H., Matsuzaki, S., Katayama, T., Tohyama, M., Ito, A., 2014. DISC1 (Disrupted-

in-Schizophrenia-1) regulates differentiation of oligodendrocytes. PLoS One 9, 1–11. https://doi.org/10.1371/journal.pone.0088506

Jadasz, J.J., Kremer, D., Göttle, P., Tzekova, N., Domke, J., Rivera, F.J., Adjaye, J., Hartung, H.P., Aigner, L., Küry, P., 2013. Mesenchymal Stem Cell Conditioning Promotes Rat Oligodendroglial Cell Maturation. PLoS One 8, 1–11. https://doi.org/10.1371/journal.pone.0071814

Jordan, C.A., Friedrich, V.L., de Ferra, F., Weismiller, D.G., Holmes, K. V, Dubois-Dalcq, M., 1990. Differential exon expression in myelin basic protein transcripts during central nervous system (CNS) remyelination. Cell Mol Neurobiol 10, 3–18. https://doi.org/10.1007/BF00733631

Kadriu, B., Greenwald, M., Henter, I.D., Gilbert, J.R., Kraus, C., Park, L.T., Jr, C.A.Z., 2021. Ketamine and Serotonergic Psychedelics : Common Mechanisms Underlying the Effects of Rapid-Acting Antidepressants. International Journal of Neuropsychopharmacology 24, 8–21. https://doi.org/10.1093/ijnp/pyaa087

Khine, A.A., Mokwena, K.E., Huma, M., Fernandes, L., 2015. Identifying the composition of street drug nyaope using two different mass spectrometer methods. Afr J Drug Alcohol Stud 14, 49–56.

Khine, Aye Aye, Elizabeth Mokwena, K., Khine, A A, 2016. “NYAOPE” in South Africa: A mini-review. Afr J Drug Alcohol Stud 15.

Koob, G.F., 2020. Neurobiology of Opioid Addiction: Opponent Process, Hyperkatifeia, and Negative Reinforcement. Biol Psychiatry 87, 44–53. https://doi.org/10.1016/j.biopsych.2019.05.023

Koob, G.F., 2010. Focus on: Neuroscience and treatment: the potential of neuroscience to inform treatment. Alcohol Res Health 33, 144–51.

Koob, G.F., 2008. A Role for Brain Stress Systems in Addiction. Neuron 59, 11–34. https://doi.org/10.1016/j.neuron.2008.06.012

Koob, G.F., Le Moal, M., 2008. Addiction and the brain antireward system. Annu Rev Psychol 59, 29–53. https://doi.org/10.1146/annurev.psych.59.103006.093548

Koob, G.F., Moal, M. Le, 2005. Neurobiology of Addiction. Neurobiology of Addiction 62, 1–490. https://doi.org/10.1016/B978-0-12-419239-3.X5036-X

Koob, G.F., Stinus, L., Moal, M. Le, Bloom, F.E., 1989. Opponent process theory of motivation: Neurobiological evidence from studies of opiate dependence. Neurosci Biobehav Rev 13, 135–140. https://doi.org/10.1016/S0149-7634(89)80022-3

Koob, G.F., Volkow, N.D., 2016. Neurobiology of addiction: a neurocircuitry analysis. Lancet Psychiatry 3, 760–773. https://doi.org/10.1016/S2215-0366(16)00104-8

Kurth, A.E., Cherutich, P., Conover, R., Chhun, N., Bruce, R.D., Lambdin, B.H., 2018. The Opioid Epidemic in Africa and Its Impact. Curr Addict Rep 5, 428–453. https://doi.org/10.1007/s40429-018-0232-9

Laule, C., Vavasour, I.M., Kolind, S.H., Li, D.K.B., Traboulsee, T.L., Moore, G.R.W., Mackay, A.L., 2007. Magnetic Resonance Imaging of Myelin. Neurotherapeutics 4, 460–484.

Laulin, J.P., Larcher, A., Célèrier, E., Le Moal, M., Simonnet, G., 1998. Long-lasting increased pain sensitivity in rat following exposure to heroin for the first time. European Journal of Neuroscience 10, 782–785. https://doi.org/10.1046/j.1460-9568.1998.00083.x

Lindner, M., Heine, S., Haastert, K., Garde, N., Fokuhl, J., Linsmeier, F., Grothe, C., Baumgärtner, W., Stangel, M., 2008. Sequential myelin protein expression during remyelination reveals fast and efficient repair after central nervous system demyelination. Neuropathology and Applied Neurobiology 34, 105–114. https://doi.org/10.1111/j.1365-2990.2007.00879.x

Lindner, M, Heine, S., Haastert, K., Garde, N., Fokuhl, J., Linsmeier, F., Grothe, C., Baumgärtner, W., Stangel, M., 2008. Sequential myelin protein expression during remyelination reveals fast and efficient repair after central nervous system demyelination. Neuropathol Appl Neurobiol 34, 105–114. https://doi.org/10.1111/j.1365-2990.2007.00879.x

Liu, L.W., Lu, J., Wang, X.H., Fu, S.K., Li, Q., Lin, F.Q., 2013. Neuronal apoptosis in morphine addiction and its molecular mechanism. Int J Clin Exp Med 6, 540–545.

Ludwin, S.K., Sternberger, N.H., 1984. An immunohistochemical study of myelin proteins during remyelination in the central nervous system. Acta Neuropathol 63, 240–248. https://doi.org/10.1007/BF00685250

Lundgaard, I., Luzhynskaya, A., Stockley, J.H., Wang, Z., Evans, K.A., Swire, M., Volbracht, K., Gautier, H.O.B., Franklin, R.J.M., ffrench-Constant, C., Attwell, D., Káradóttir, R.T., 2013. Neuregulin and BDNF Induce a Switch to NMDA Receptor-Dependent Myelination by Oligodendrocytes. PLoS Biology 11. https://doi.org/10.1371/journal.pbio.1001743

Ly, C., Greb, A.C., Cameron, L.P., Wong, J.M., Barragan, E. V., Wilson, P.C., Burbach, K.F., Soltanzadeh Zarandi, S., Sood, A., Paddy, M.R., Duim, W.C., Dennis, M.Y., McAllister, A.K., Ori-McKenney, K.M., Gray, J.A., Olson, D.E., 2018. Psychedelics Promote Structural and Functional Neural Plasticity. Cell Rep 23, 3170–3182. https://doi.org/10.1016/j.celrep.2018.05.022

Maier, O., Hoekstra, D., Baron, W., 2008. Polarity development in oligodendrocytes: Sorting and trafficking of myelin components. Journal of Molecular Neuroscience 35, 35–53. https://doi.org/10.1007/s12031-007-9024-8

Maillet, E.L., Milon, N., Heghinian, M.D., Fishback, J., Schürer, S.C., Garamszegi, N., Mash, D.C., 2015. Noribogaine is a G-protein biased κ-opioid receptor agonist. Neuropharmacology 99, 675–688. https://doi.org/10.1016/j.neuropharm.2015.08.032

Marton, S., González, B., Rodríguez-Bottero, S., Miquel, E., Martínez-Palma, L., Pazos, M., Pedro Prieto, J., Rodríguez, P., Sames, D., Seoane, G., Scorza, C., Cassina, P., Carrera, I., 2019. Ibogaine administration modifies GDNF and BDNF expression in brain regions involved in mesocorticolimbic and nigral dopaminergic circuits. Front Pharmacol 10, 1–13. https://doi.org/10.3389/fphar.2019.00193

Mash, D.C., Kovera, C.A., Buck, B.E., Norenberg, M.D., Shapshak, P., Lee Hearn, W., Sanchez-Ramos, J., 1998. Medication development of ibogaine as a pharmacotherapy for drug

dependence, in: Annals of the New York Academy of Sciences. pp. 274–292. https://doi.org/10.1111/j.1749-6632.1998.tb08242.x

Mei, F., Mayoral, S.R., Nobuta, H., Wang, F., Desponts, C., Lorrain, D.S., Xiao, L., Green, A.J., Rowitch, D., Whistler, J., Chan, J.R., 2016. Identification of the kappa-opioid receptor as a therapeutic target for oligodendrocyte remyelination. Journal of Neuroscience 36, 7925–7935. https://doi.org/10.1523/JNEUROSCI.1493-16.2016

Mendes, F.R., Costa, C. dos S., Wiltenburg, V.D., Morales-Lima, G., Fernandes, J.A.B., Filev, R., 2022. Classic and non-classic psychedelics for substance use disorder: A review of their historic, past and current research. Addiction Neuroscience 3, 100025. https://doi.org/10.1016/j.addicn.2022.100025

Miguel-Hidalgo, J.J., 2018. Molecular neuropathology of astrocytes and oligodendrocytes in alcohol use disorders. Front Mol Neurosci. https://doi.org/10.3389/fnmol.2018.00078

Morgan, P.L., Wang, Y., 2019. The opioid epidemic, neonatal abstinence syndrome, and estimated costs for special education services. Am J Manag Care 25, S264–S269.

Mthembi, P.M., Mwenesongole, E.M., Cole, M.D., 2018. Chemical profiling of the street cocktail drug 'nyaope' in South Africa using GC–MS I: Stability studies of components of 'nyaope' in organic solvents. Forensic Sci Int 292, 115–124. https://doi.org/10.1016/j.forsciint.2018.08.001

Nathan, P.E., Conrad, M., Skinstad, A.H., 2016. History of the Concept of Addiction. Annu Rev Clin Psychol 12, 29–51. https://doi.org/10.1146/annurev-clinpsy-021815-093546

Ndlovu, N.A., Morgan, N., Malapile, S., Subramaney, U., Daniels, W., Naidoo, J., van den Heuvel, M.P., Calvey, T., 2021. Fronto-temporal cortical atrophy in 'nyaope' combination heroin and cannabis use disorder. Drug Alcohol Depend 221. https://doi.org/10.1016/j.drugalcdep.2021.108630

Oberoi, R., Chu, T., Mellen, N., Jagadapillai, R., Ouyang, H., Devlin, L.A., Cai, J., 2019. Diverse changes in myelin protein expression in rat brain after perinatal methadone exposure. Acta Neurobiol Exp (Wars) 79, 367–373. https://doi.org/10.21307/ane-2019-034

Pedraza, L., Fidler, L., Staugaitis, S.M., Colman, D.R., 1997. The active transport of myelin basic protein into the nucleus suggests a regulatory role in myelination. Neuron 18, 579–589. https://doi.org/10.1016/S0896-6273(00)80299-8

Peltz, G., Südhof, T.C., 2018. The neurobiology of opioid addiction and the potential for prevention strategies. JAMA - Journal of the American Medical Association 319, 2071–2072. https://doi.org/10.1001/jama.2018.3394

Peltzer, K., Davids, A., Njuho, P., 2011. Alcohol use and problem drinking in South Africa. Afr J Psychiatry (Johannesbg) 1, 30–37.

Pliiddemann, A., Parry, C.D.H., Flisher, A.J., Jordaan, E., 2008. Heroin Users in Cape Town, South Africa: Injecting Practices, HIV-Related Risk Behaviors, and Other Health Consequences. J Psychoactive Drugs 40, 273–279. https://doi.org/10.1080/02791072.2008.10400642

Popik, P., Layer, R.T., Skolnick, P., 1994. The putative anti-addictive drug ibogaine is a competitive inhibitor of [3H]MK-801 binding to the NMDA receptor complex. Psychopharmacology (Berl) 114, 672–674. https://doi.org/10.1007/BF02245000

Pothos, E., Rada, P., Mark, G.P., Hoebel, B.G., 1991. Dopamine microdialysis in the nucleus accumbens during acute and chronic morphine, naloxone-precipitated withdrawal and clonidine treatment. Brain Res 566, 348–350. https://doi.org/10.1016/0006-8993(91)91724-F

Ray, S.K., Matzelle, D.D., Sribnick, E.A., Guyton, M.K., Wingrave, J.M., Banik, N.L., 2003. Calpain inhibitor prevented apoptosis and maintained transcription of proteolipid protein and myelin basic protein genes in rat spinal cord injury, in: Journal of Chemical Neuroanatomy. Elsevier, pp. 119–124. https://doi.org/10.1016/S0891-0618(03)00044-9

Razoux, F., Garcia, R., Léna, I., 2007. Ketamine, at a dose that disrupts motor behavior and latent inhibition, enhances prefrontal cortex synaptic efficacy and glutamate release in the nucleus accumbens. Neuropsychopharmacology 32, 719–727. https://doi.org/10.1038/sj.npp.1301057

Rezvani, A.H., Overstreet, D.H., Leef, Y.W., 1995. Attenuation of alcohol intake by Ibogaine in three strains of alcohol-preferring rats. Pharmacol Biochem Behav 52, 615–620. https://doi.org/10.1016/0091-3057(95)00152-M

Rossetti, Z.L., Hmaidan, Y., Gessa, G.L., 1992. Marked inhibition of mesolimbic dopamine release: a common feature of ethanol, morphine, cocaine and amphetamine abstinence in rats. Eur J Pharmacol 221, 227–234. https://doi.org/10.1016/0014-2999(92)90706-A

Ruskamo, S., Raasakka, A., Pedersen, J.S., Martel, A., Škubník, K., Darwish, T., Porcar, L., Kursula, P., 2022. Human myelin proteolipid protein structure and lipid bilayer stacking. Cellular and Molecular Life Sciences 79, 1–19. https://doi.org/10.1007/s00018-022-04428-6

Saab, A.S., Tzvetavona, I.D., Trevisiol, A., Baltan, S., Dibaj, P., Kusch, K., Möbius, W., Goetze, B., Jahn, H.M., Huang, W., Steffens, H., Schomburg, E.D., Pérez-Samartín, A., Pérez-Cerdá, F., Bakhtiari, D., Matute, C., Löwel, S., Griesinger, C., Hirrlinger, J., Kirchhoff, F., Nave, K.A., 2016. Oligodendroglial NMDA Receptors Regulate Glucose Import and Axonal Energy Metabolism. Neuron 91, 119–132. https://doi.org/10.1016/j.neuron.2016.05.016

Saal, D., Dong, Y., Bonci, A., Malenka, R.C., 2003. Erratum: Drugs of abuse and stress trigger a common synaptic adaptation in domamine neurons (Neuron (February 20, 2003) 37 (577-582)). Neuron 38, 359. https://doi.org/10.1016/S0896-6273(03)00208-3

Skripuletz, T., Gudi, V., Hackstette, D., Stangel, M., 2011. De- and remyelination in the CNS white and grey matter induced by cuprizone: The old, the new, and the unexpected. Histol Histopathol. https://doi.org/10.14670/HH-26.1585

Soriani, O., Kourrich, S., 2019. The Sigma-1 Receptor: When Adaptive Regulation of Cell Electrical Activity Contributes to Stimulant Addiction and Cancer. Front Neurosci. https://doi.org/10.3389/fnins.2019.01186

Steelman, A.J., Zhou, Y., Koito, H., Kim, S.J., Payne, H.R., Lu, Q.R., Li, J., 2016. Activation of oligodendroglial Stat3 is required for efficient remyelination. Neurobiol Dis 91, 336–346. https://doi.org/10.1016/j.nbd.2016.03.023

Uhl, G.R., Koob, G.F., Cable, J., 2019. The neurobiology of addiction. Ann N Y Acad Sci 1451, 5–28. https://doi.org/10.1111/nyas.13989

Uyeda, A., Muramatsu, R., 2020. Molecular mechanisms of central nervous system axonal regeneration and remyelination: A review. Int J Mol Sci. https://doi.org/10.3390/ijms21218116

Vadivelu, N., Kai, A.M., Kodumudi, V., Sramcik, J., Kaye, A.D., 2018. The Opioid Crisis: a Comprehensive Overview. Curr Pain Headache Rep 22, 1–6. https://doi.org/10.1007/s11916-018-0670-z

Verrier, J.D., Jackson, T.C., Gillespie, D.G., Janesko-Feldman, K., Bansal, R., Goebbels, S., Nave, K.A., Kochanek, P.M., Jackson, E.K., 2013. Role of CNPase in the oligodendrocytic extracellular 2′,3′-cAMP-adenosine pathway. GLIA 61, 1595–1606. https://doi.org/10.1002/glia.22523

Volkow, N.D., Wang, G.J., Telang, F., Fowler, J.S., Logan, J., Jayne, M., Ma, Y., Pradhan, K., Wong, C., 2007. Profound decreases in dopamine release in striatum in detoxified alcoholics: Possible orbitofrontal involvement. Journal of Neuroscience 27, 12700–12706. https://doi.org/10.1523/JNEUROSCI.3371-07.2007

Wang, X., Loram, L.C., Ramos, K., De Jesus, A.J., Thomas, J., Cheng, K., Reddy, A., Somogyi, A.A., Hutchinson, M.R., Watkins, L.R., Yin, H., 2012. Morphine activates neuroinflammation in a manner parallel to endotoxin. Proc Natl Acad Sci U S A 109, 6325–6330. https://doi.org/10.1073/pnas.1200130109

Wegener, A., Deboux, C., Bachelin, C., Frah, M., Kerninon, C., Seilhean, D., Weider, M., Wegner, M., Nait-Oumesmar, B., 2015. Gain of Olig2 function in oligodendrocyte progenitors promotes remyelination. Brain 138, 120–135. https://doi.org/10.1093/brain/awu375

Weiss, F., Ciccocioppo, R., Parsons, L.H., Katner, S., Liu, X.I.U., Zorrilla, E.P., Valdez, G.R., Ben-Shahar, O., Angeletti, S., Richter, R.R., 2001. Compulsive drug-seeking behavior and relapse: Neuroadaptation, stress, and conditioning factors. Ann N Y Acad Sci 937, 1–26. https://doi.org/10.1111/j.1749-6632.2001.tb03556.x

Weiss, F., Markou, A., Lorang, M.T., Koob, G.F., 1992. Basal extracellular dopamine levels in the nucleus accumbens are decreased during cocaine withdrawal after unlimited-access self-administration. Brain Res 593, 314–318. https://doi.org/10.1016/0006-8993(92)91327-B

Xiao, J., Kilpatrick, T.J., Murray, S.S., 2009. The role of neurotrophins in the regulation of myelin development. Neurosignals 17, 265–276. https://doi.org/10.1159/000231893

Yang, T., Zheng, Q., Wang, S., Fang, L., Liu, L., Zhao, H., Wang, L., Fan, Y., 2017. Effect of catalpol on remyelination through experimental autoimmune encephalomyelitis acting to promote Olig1 and Olig2 expressions in mice. BMC Complement Altern Med 17, 1–15. https://doi.org/10.1186/s12906-017-1642-2

Zhang, S., Zhu, X., Gui, X., Croteau, C., Song, L., Xu, J., Wang, A., Bannerman, P., Guo, F., 2018. Sox2 is essential for oligodendroglial proliferation and differentiation during postnatal brain myelination and CNS remyelination. Journal of Neuroscience 38, 1802–1820. https://doi.org/10.1523/JNEUROSCI.1291-17.2018

Zhao, C., Ma, D., Zawadzka, M., Fancy, S.P.J., Elis-Williams, L., Bouvier, G., Stockley, J.H., de Castro, G.M., Wang, B., Jacobs, S., Casaccia, P., Franklin, R.J.M., 2015. Sox2 sustains recruitment of oligodendrocyte progenitor cells following CNS demyelination and primes them for differentiation during remyelination. Journal of Neuroscience 35, 11482–11499. https://doi.org/10.1523/JNEUROSCI.3655-14.2015

Zhao, H., Gao, X.Y., Liu, Z.H., Lin, J.W., Wang, S.P., Wang, D.X., Zhang, Y.B., 2019. Effects of the transcription factor Olig1 on the differentiation and remyelination of oligodendrocyte precursor cells after focal cerebral ischemia in rats. Mol Med Rep 20, 4603–4611. https://doi.org/10.3892/mmr.2019.10713

A1. Ethics Clearance Certificate

ANIMALS RESEARCH ETHICS COMMITTEE (AREC)

UNIVERSITY OF THE WITWATERSRAND, JOHANNESBURG

STRICTLY CONFIDENTIAL

CLEARANCE CERTIFICATE NUMBER: 2021/05/01/C

APPLICANT: Ms D Govender
School: School of Anatomical Sciences; Department: N/A; Location: WRAF

PROJECT TITLE: The effects of ibogaine on myelination in the white matter of Sprague-Dawley rats
Category: C; Species and Numbers involved: *50X post-natal day 42/230 - 250g, male, Sprague Dawley Rats*

Approval is hereby given for the use of animals for the research project named above and described in the application reviewed by a quorate meeting of the AREC held on 25 May 2021. This approval remains valid until 13 Jun 2023 and is conditional to the following (if blank there are no special conditions):

Condition 1	Condition 2	Condition 3	Condition 4

All material changes to the approved research must be reported to the AREC before they are implemented. Failure to do so will invalidate this clearance certificate.

An annual progress report must be provided to the AREC.

The use of these animals is subject to AREC guidelines on the use and care of laboratory animals, is limited to the procedures described in the application and is subject to additional conditions listed below:

I, the Chair of the AREC (or my designated representative) am satisfied that the proposed research is ethical as judged by local law, international standards and University policy.

Signed: _____ _____ Date: ____14/06/2021_____
(Chairperson of the AREC)

I am satisfied that the persons listed in this application are competent to perform the procedures described in the application, in the context of Section 23 (1) (c) of the veterinary and Para-veterinary Professions Act (19 of 1982).

CC: Student supervisor: «Title1» «Initials1» «Supervisor_surname»
Director Wits Research Animal Facility (WRAF): Dr Kim Jardine

ANIMALS RESEARCH ETHICS COMMITTEE (AREC)

UNIVERSITY OF THE WITWATERSRAND, JOHANNESBURG

Signed: __ _____ Date: _14 June 2021_____
(Registered Veterinarian)

A1.1 Modification and extensions

A1.1.1: M&E for added researcher

AREC 2017 M&E

Please note that only typewritten applications will be accepted.

UNIVERSITY OF THE WITWATERSRAND
ANIMAL RESEARCH ETHICS COMMITTEE
MODIFICATIONS AND EXTENSIONS TO EXPERIMENTS

a. Name: Demi Govender

b. School and email address: School of anatomical sciences

1444170@students.wits.ac.za

c. Experiment to be modified / extended **AREC/AESC NO**

Original AESC number	**2021**	**05**	**01C**
Other M&Es :			

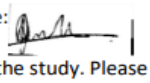
d. Project Title: The effects of ibogaine on myelination in the white matter of Sprague-Dawley rats

		No.	**Species**
e.	Number and species of animals originally approved:	50	*Sprague-dawley rats*
f.	Number of additional animals previously allocated on M&Es:	0	*Sprague-dawley rats*
g.	Total number of animals allocated to the experiment to date:	50	*Sprague-dawley rats*
h.	Number of animals used to date:	10	*Sprague-dawley rats*

i. Specific modification / extension requested:
Leila Moloko (1155553) added to certificate as a co-worker

j. Motivation for modification / extension:

Leila needs to be added as animal brain tissue will be collected for her masters project.

Date: 19/08/2021 Signature: 

RECOMMENDATIONS
Approval of MSc student, Leila Moloko, as a co-worker on the study. Please note: Should the newly assigned co-worker be involve with animal handling then they are required to attend the WRAF orientation course prior to initiating any animal work. Please contact Dr Kim Jardine for details. (kimberly.jardine@wits.ac.za)

Date:20 August 2021 Signature: 
Deputy-Chair, AREC

A1.1.2 M&E for Change in Doses of Escalated Morphine Regimen

AREC 2017 M&E

Please note that only typewritten applications will be accepted.

UNIVERSITY OF THE WITWATERSRAND

ANIMAL RESEARCH ETHICS COMMITTEE

MODIFICATIONS AND EXTENSIONS TO EXPERIMENTS

a. Name: Demi Govender

b. School and email address: School of anatomical sciences

1444170@students.wits.ac.za

c. Experiment to be modified / extended **AREC/AESC NO**

Original AESC number	**2021**	**05**	**01C**
Other M&Es :			2

d. Project Title: The effects of ibogaine on myelination in the white matter of Sprague-Dawley rats

		No.	**Species**
e.	Number and species of animals originally approved:	50	*Sprague-dawley rats*
f.	Number of additional animals previously allocated on M&Es:	10	*Sprague-dawley rats*
g.	Total number of animals allocated to the experiment to date:	60	*Sprague-dawley rats*
h.	Number of animals used to date:	33	*Sprague-dawley rats*

i. Specific modification / extension requested:

I would like to change the escalated morphine regimen from doses of 5mg/kg for 2 days, 10 mg/kg for 2 days, 15mg/kg for 2 days, 20mg/kg for 2 days and 25mg/kg for 2 days to an escalated morphine regimen of 5mg/kg for 2 days, 7,5mg/kg for 3 days, 10mg/kg for 3 days and 15mg/kg for 2 days.

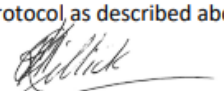
j. Motivation for modification / extension:

The change will decrease the amount of morphine received and keeping the highest dose at 15mg/kg. This will allow the animals more time to adapt to the increasing morphine doses as it is over 3 days with a 2,5mg/kg increment rather than 5mg/kg. This was discussed with Dr. Kim Jardine and Dr Tanya Calvey.

Date: 13/04/2022 Signature: 

RECOMMENDATIONS

Approval for the modification of the morphine dose escalation protocol as described above.

Date:19 April 2022 Signature: 

Deputy Chair, AREC

A1.1.3 Additional SD Rats Requested

AREC 2017 M&E

Please note that only typewritten applications will be accepted.

UNIVERSITY OF THE WITWATERSRAND
ANIMAL RESEARCH ETHICS COMMITTEE
MODIFICATIONS AND EXTENSIONS TO EXPERIMENTS

a. Name: Demi Govender

b. School and email address: School of anatomical sciences

1444170@students.wits.ac.za

c. Experiment to be modified / extended

			AREC/AESC NO
Original AESC number	2021	05	01C
Other M&Es :			1

d. Project Title: The effects of ibogaine on myelination in the white matter of Sprague-Dawley rats

		No.	Species
e.	Number and species of animals originally approved:	50	*Sprague-dawley rats*
f.	Number of additional animals previously allocated on M&Es:	0	*Sprague-dawley rats*
g.	Total number of animals allocated to the experiment to date:	50	*Sprague-dawley rats*
h.	Number of animals used to date:	20	*Sprague-dawley rats*

i. Specific modification / extension requested:
I would like to request 10 additional male Sprague-Dawley rats, PND 42-45.

j. Motivation for modification / extension:
The last group of rats had 4 deaths due to pulmonary effusion, this incident was reported in an incident report DATA. The initial advice from the vet was to lower the morphine dose and thus this group received different treatments to our protocol. We would like to redo this group using the escalated morphine regimen as stated in my application, but to avoid deaths we will use more litters for genetic variation. Three of the deaths were from the same litter. The rats in this group were also smaller than the first group of rats we used.

There should have not been deaths at such a low dose, as other experiments have used much higher doses of morphine within the same species, age range and sex (Liu et al., 2013; Nylander et al., 1995; Rane and Ask, 1992). Also morphine does not cause pulmonary effusion so it is unlikely that the morphine treatment was the cause of death.

This group is very important for accurate comparison of the genetic and protein analyses. We therefore request an additional 10 rats in order to redo this specific group.

Liu, L.W., Lu, J., Wang, X.H., Fu, S.K., Li, Q., Lin, F.Q., 2013. Neuronal apoptosis in morphine addiction and its molecular mechanism. Int. J. Clin. Exp. Med. 6, 540–545.
Nylander, I., Vlaskovska, M., Terenius, L., 1995. The effects of morphine treatment and morphine withdrawal on the dynorphin and enkephalin systems in sprague-dawley rats.

AREC 2017 M&E

Psychopharmacology (Berl). 118, 391–400. https://doi.org/10.1007/BF02245939.
Rane, A., Ask, B., 1992. A conspicuous down-regulating effect of morphine on essential steroid hydroxylation reactions and certain drug N-demethylations. J. Steroid Biochem. Mol. Biol. 41, 91–98. https://doi.org/10.1016/0960-0760(92)90229-C

Date: 28/10/2021 Signature:

RECOMMENDATIONS
Approval for the additional 10 rats to the study however, the committee recommends a staggered approach where 2 to 3 animals receive the treatment at a time so as to limit any potential mortality should it occur at the new morphine concentration.

Date: 2 March 2022 Signature:

Deputy Chair, AREC

A2 Additional Methods

A2.1 Morphine protocol adjustments

The morphine protocol was adjusted to decrease the doses of the morphine given to the rats as too many had died from the first protocol (detailed in section 3.1). Once the adjustment was done, we did notice that the morphine even at low doses made the rats limp and bury their heads in the sawdust. This is believed to have cause suffocation in some of the initial rats. We changed their cages from sawdust to paper to avoid this and did not have any lung related deaths (pulmonary oedema) since the change in cage material.

A2.2 Alternative Protein Extraction Protocol

Two methods were tested for protein extraction to make sure we were able to extract the most amount of total protein from the small amount of white matter tissue that was harvested. The first method used was homogenising the brain tissue in phosphate buffered saline (PBS) 5 times for 15 seconds at 5000 rpm with 5 seconds rest. The second method used only the lower organic phase which contained the proteins from the Qiazol lysis homogenate described previously. Ice cold acetone was added to the proteins and left overnight in the freezer to precipitate the proteins from the Qiazol lysis mixture. The acetone precipitate was centrifuged at 14500 rpm for 10 minutes and the supernatant was discarded. The pellet was airdried on ice in the Eppendorf tube for 10 minutes. This pellet was then homogenised with either PBS or 5% sodium dodecyl sulphate (SDS). We homogenised in two buffers to determine which solution solubilized the pellet better this showed no difference in concentration of total protein yield as seen in table 3 but visually the SDS method was a more homogenous mixture. The two methods were compared using a BCA assay to determine total protein concentration. The BCA showed that the protein concentrations did not differ between the two methods thus we chose to continue with the Qiazol lysis method as we could use the same tissue for both proteins and RNA as seen in table 3. This was needed as the white matter harvested from the brains was limited.

Table 3: Comparison of concentrations in total protein yield using different protein extraction methods

Sample Number	Method	BCA Concentration (µg/ml)
27	Homogenised in PBS	856.209
27	Qiazol lysis method homogenised in PBS	894.200
24	Homogenised in PBS	843.167
24	Qiazol lysis method homogenised in PBS	682.696
21	Qiazol lysis method homogenised in 5% SDS	1825.473
23	Qiazol lysis method homogenised in 5% SDS	2067.340
22	Qiazol lysis method homogenised in PBS	1772.565

A2.3 Plasmid Preparation for standard curve of qPCR

A standard curve is used in qPCR to measure the amount of a gene present in an unknown sample. The standard curve is obtained by taking known amounts of plasmid DNA of a target gene and making serial dilutions. The plasmid DNA for the standard curve were assembled using DNA obtained by amplification of MBP, PLP, and CNP coding sequences. The primer sets are listed in table 2, in the methods section 3.5. The reaction using the 2x Taq DNA polymerase Master Mix (Ampliqon, Denmark) was done at 95°C for 5 minutes, 30 cycles of 95°C for 20 seconds, 51°C for 20 seconds,72°C for 30 seconds and ended with 72°C for 7 minutes using the. This was run on a 1% agarose gel. The DNA was excised from the gel after viewing the bands using a UVP tabletop Transilluminator (California, USA) for a short period of time as an imaging doc using high levels of UV can damage the DNA. The excised gel was weighed and dissolved in 3 volumes of GQ buffer from the minElute gel extraction kit (Qiagen, Netherlands). This was incubated at 50°C for 10 minutes for the gel to dissolve. The solution was yellow which indicated the pH was within range. 1 gel volume of isopropanol was added and the Eppendorf tube was inverted. This was added to the minElute column and centrifuged for 1 minute, flowthrough was discarded. QG buffer was added and then the column was washed with PE buffer. The DNA was eluted with elution buffer. The DNA concentration was measured using the Thermo Scientific Nanodrop™ ND-1000 (Massachusetts, USA).

The DNA was then cloned using the TOPO vector from the TOPO® TA Cloning® Kit for Sequencing (Invitrogen, Massachusetts, USA). A cloning reaction of PCR product, salt solution and vector was added to competent cells and mixed gently. The reaction was incubated on ice for 10 minutes and heat shocked at 42°C for 30 seconds. Room temperature SOC (Super Optimal broth with Catabolite repression) medium (Thermofischer Scientific, Massachusetts, United States) was added and then shook at 200 rpm for 20 minutes at 37°C. The SOC medium provides a nutrient rich environment for the cells to grow. This was then spread onto a Lysogenia Broth (LB) agar carbenicillin plates plate and incubated overnight at 37°C.

A bacterial colony from each plate was selected and cultured in LB broth that contained carbenicillin (100 µg/ml). The culture was incubated for 12-16 hours at 37°C. The culture was centrifuged to pellet the bacterial cells. The ZR Plasmid Miniprep Classic (Zymo Research, California, USA) was used to extract the plasmid DNA. P1 buffer was added to the bacterial pellet and vortexed to resuspend them. P2 buffer was added and inverted to lyse the cells. P3 buffer was added to neutralise the solution and form a green precipitate with the K-SDS and cell debris. The supernatant was transferred to the column without disturbing the pellet and centrifuged at 11000g for 30 seconds. Flow through was discarded and endowash was added to the column and centrifuged. The plasmid wash was subsequently added and centrifuged. DNA elution buffer was added, and the DNA is collected an Eppendorf tube. The DNA was measured using the Thermo Scientific Nanodrop™ ND-1000 (Massachusetts, USA). The plasmids were checked for correct DNA insertion as described in section A2.3.1.

Table 4: Concentration of PLasmids

Plasmid	Concentration of DNA (ng/µl)	260/280	260/230
CNP	134,6	1,84	1,47
MBP	160,0	1,90	1,58
PLP	94,8	1,86	1,29

Serial dilutions were made and tested to see when the samples would fall within the standard curve concentrations. The first set of serial dilutions of the standard curve were 10 ng/µl, 2 ng/µl, 0,4 ng/µl and 0,08 ng/µl (Figure 12). This showed none of the samples falling within the curve thus we adjusted it to 0,4 ng/µl, 0,04 ng/µl, 4 pg/µl, 0,4 pg/µl (figure 13). This standard

curve was still too large for the samples values to fall within so we moved onto the femtogram standard curve with 400 fg/µl, 40 fg/µl, 4 fg/µl and 0,4 fg/µl (figure 14). This curve was adjusted to the curves in table 4.

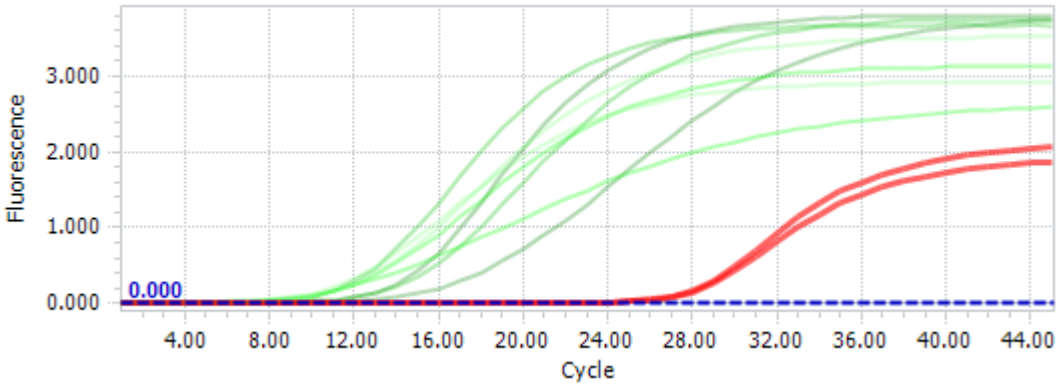


Figure 13: CNP standard curve of 10ng/µl to 0.08ng/µl. The green curves are the standard curve values. The red curves are the test samples that were used. This shows that the samples do not fall within the curve.

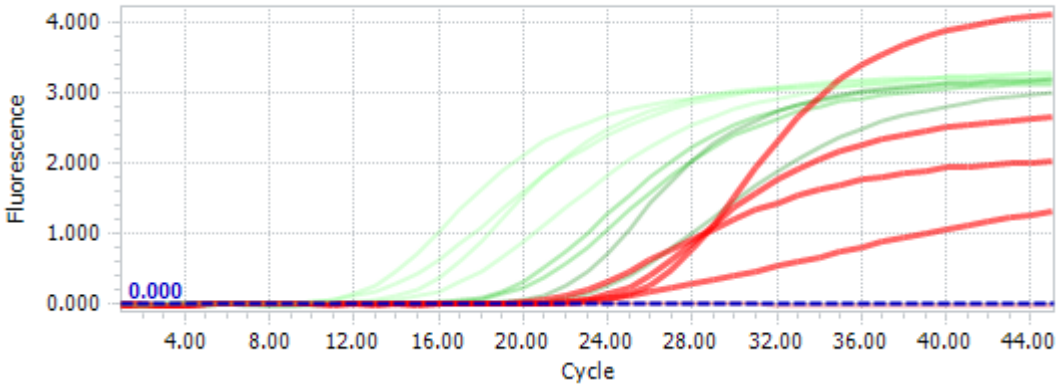


Figure 13: CNP standard curve of 0,4 ng/µl to 0,4 pg/µl. The green curves are the standard curve values. The red curves are the test samples that were used. This shows that the samples do not fall within the curve.

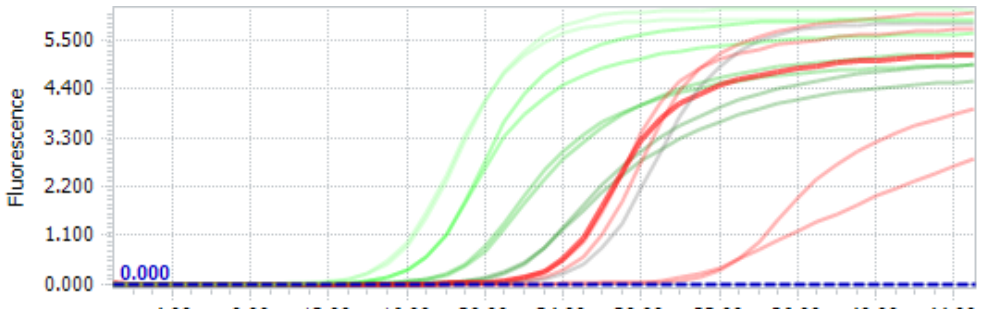
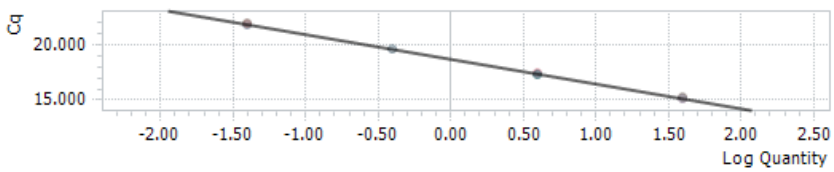
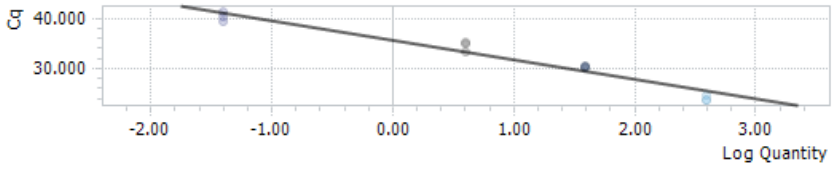
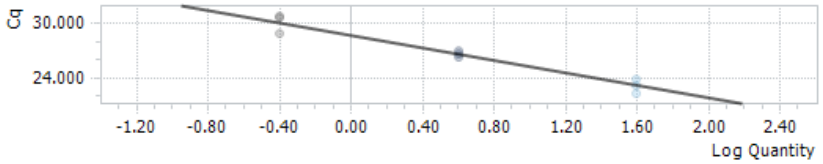


Figure 14: CNP standard curve of 400 fg/ul to 0,4 fg/ul. The green curves are the standard curve values. The red curves are the test samples that were used. This shows that some samples fall within the curve but one further dilution was needed.

Table 5: Serial dilutions for standard curve

Gene	Curve Equation	Standard curve dilutions (femtograms)	Standard curve from saline group
CNP (247 bp)	Y=-2.23x+18.65 R^2=1	40 – 4 - 0,4 - 0,04	
MBP (263 bp)	Y=-3.94x+35.51 R^2=0.96	400 – 40 - 4 - 0,4- 0,04	
PLP (284 bp)	Y=-3.52x+28.67 R^2=0.95	40 - 4 - 0,4 - 0,04	

A2.3.1 Plasmid Checks for the correct sequence amplification

A2.3.1.1 Restriction Enzyme Digest

Restriction enzyme digest was done to check that the correct DNA sequence was added to the plasmid. Restriction enzymes are naturally occurring enzymes that cleave DNA at specific sequences. We used NCO1 and ECOR1 restriction enzymes (Thermofischer Scientific, Massachusetts, United States) as these had predicted cut sites in the TOPO vector used. The NCO1 was predicted to cut the vector once and the ECOR1 enzyme cut the vector twice. The 20µl restriction digest reaction contained distilled water, 2 µl 10x restriction enzyme specific buffer, 1 µg plasmid DNA and 1 µl restriction enzyme (10U/µl). The reaction was incubated for 1 hour at 37°C. The samples were then loaded on a 1% agarose gel and run at 100V until the dye front reached the end of the gel.

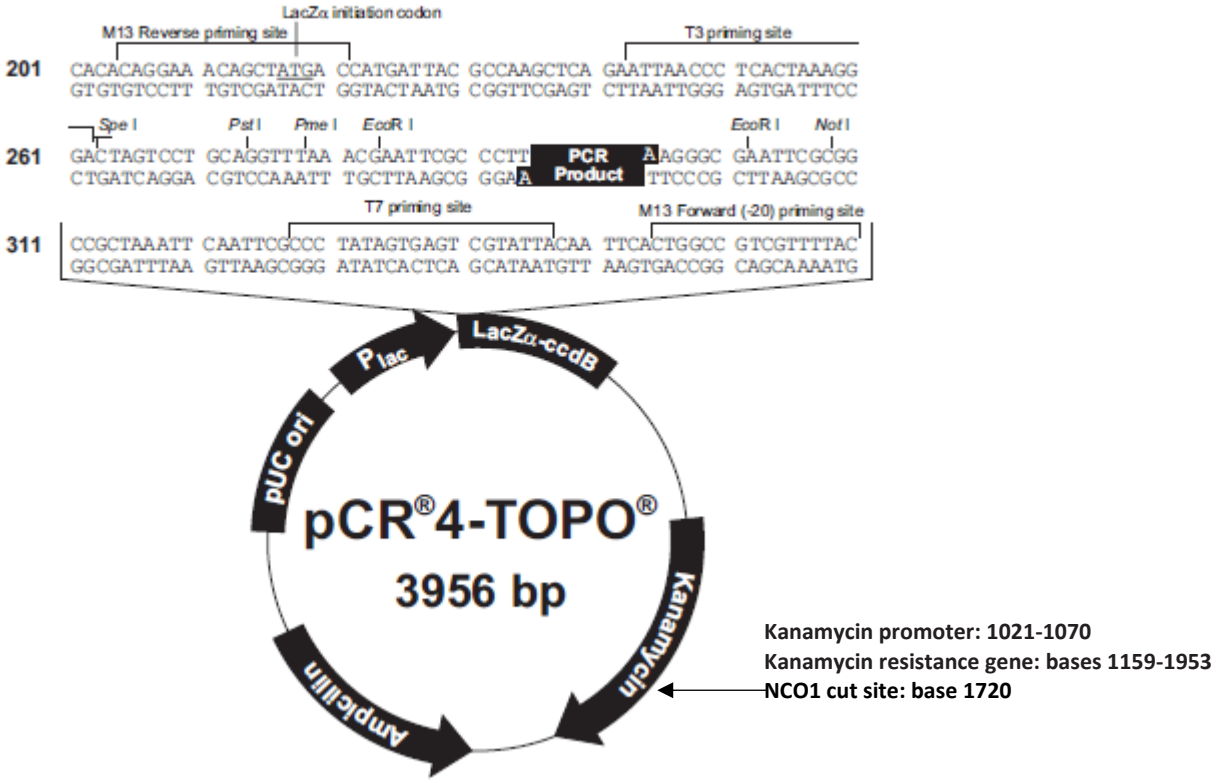


Figure 14: TOPO vector with restriction enzyme cut sites (Invitrogen life technologies, TOPO TA manual)

The restriction enzyme digest showed that the PCR product was inserted into the plasmid correctly (Figure 13). The uncut plasmid DNA has two bands one being the supercoiled DNA at 4000 bp on the gel and the other at approximately 8000bp is the open circular DNA. The ECOR1 digests showed two bands implying two cuts were made on either side of the insert as depicted in figure 12. The second band appears very low in the gel as the DNA inserts are very small fragments as shown by the arrows in figure 13 usually appearing after the 1000bp marker. The CNP plasmid NCO1 digest has one big band implying one cut was made. PLP and MBP have NCO1 sites within their sequences and in the plasmid hence there are two fragments seen in figure 13.

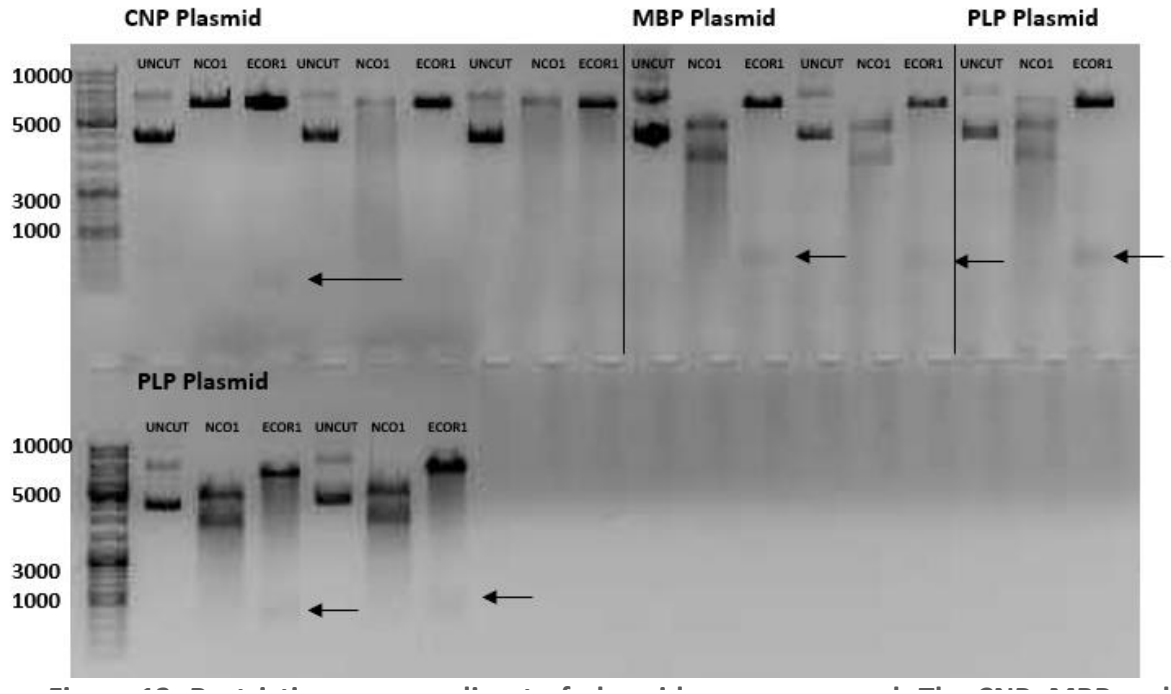


Figure 15: Restriction enzyme digest of plasmids on agarose gel. The CNP, MBP and PLP plasmids were digested with NCO1 and ECOR1. The uncut plasmid and digests were run. The arrows show the DNA insert from the ECOR1 digests as the fragments were small.

A2.3.1.2 Sequencing of Myelin Protein Plasmids

The plasmids were sequenced using the BigDye™ Terminator v3.1 Cycle Sequencing (Thermofischer Scientific, Massachusetts, United States). This was done to ensure that the correct DNA sequences were inserted into the plasmids. Each reaction in an Eppendorf tube contained 2,6 µl BigDye™ Terminator 3.1 Ready Reaction Mix (pink mix), 5,4 µl of Bioline buffer, 10 µl of plasmid DNA (400 ng), 2 µl of 2,5 µM primers. The primers used were T7 and M13 primers. Standard cycling procedures were used for the reactions in a C1000 Touch™ Thermal Cycler (Bio-Rad, USA) which was 25 cycles of: 96°C for 10 seconds, 50°C for 5 seconds, 60°C for 4 minutes and held at 4°C. The sequencing reactions were then cleaned using the sodium acetate method. 1 ml of anhydrous ethanol (EtOH) and 40µl 3M sodium acetate (NaOAc) with a pH of 4.6 were mixed together. 50 µl of the EtOH/NaOAc mixture was added to each sequencing reaction on the plate. The plate was centrifuged for 30 minutes at 2000 g. The plate was inverted onto paper towel and centrifuged for 1 minute at 150 g. 100 µl of cold ethanol was added to the wells in the plate. The plate was centrifuged for 5 minutes at 2000 g. The plate was then inverted onto paper towel and centrifuged for 1 minute at 150 g to ensure the pellets were dry. The plate was then stored at -20°C until it was

picked up to be sequenced by Inqaba Biotec™ (Pretoria, South Africa). The sequences were then run on BLAST® (BLAST: Basic Local Alignment Search Tool (nih.gov)) to confirm that all the plasmid inserts were their specific myelin gene. All plasmids were confirmed as the correct inserts by sequencing.

A2.4 Recipes for Solutions and Buffers

1. **Lysogenia Broth (LB)**

   1 g NaCl

   1 g Tryptone

   0,5 g Yeast

   Made up to 100 ml with distilled water and autoclaved.

2. **LB Agar Plate**

   5 g NaCl

   5 g Tryptone

   2,5 g Yeast

   7,5 g Agar

   Made up to 1 L with distilled water and autoclaved.

3. **Transformation Buffer for competent cells (100 mM $CaCl_2$, 10mM PIPES HCl, 15% glycerol)**

   1,4702 g $CaCl_2$

   0,3024 g PIPES HCl

   15 ml Glycerol

   Made up to 100 ml and autoclaved.

4. **Competent cells**

   Diluted culture of house made cells (pu25c): 1 ml of cells in 40 ml of LB

   Grew culture till A_{600}=0,4

   Pelleted cells at 1500 rpm for 10 minutes with a brake of 10

   Added transformation buffer to make the cells chemically competent.

   Incubated on ice for 20 minutes.

Pelleted and resuspended in 1 ml transformation buffer.

Then aliquoted cells and stored at -4°C.

5. **Monomer Solution (30% acrylamide, 2,7% bis-acrylamide)**

   73g acrylamide

   2g bisacrylamide

   Made up to 250ml with distilled water (dH_2O)

6. **Separating Gel Buffer (1,5 M Tris-HCl, pH=8,8)**

   45,37 g Tris in 200 ml dH_2O

   Adjusted with NaOH or HCl

   Made up to final volume of 250 ml.

7. **Stacking Gel Buffer (500 mM Tris-HCl, pH=6,8)**

   3 g Tris in 40 ml of dH_2O

   Adjusted with NaOH or HCl

   Made up to final volume of 50 ml.

8. **10X Tank Buffer (250 mM Tris-HCl, 192 mM glycine, 0,1% SDS, pH=8,3)**

   30 g Tris

   144 g glycine

   10 g SDS

   Made up to 1 L with dH_2O.

   This was also used for transfer buffer and made up with 20% Methanol.

9. **Reducing Sample Buffer (125mM Tris, 4% SDS, 20% glycerol, 10% β-mercaptoethanol, pH=6,8)**

   2,5 ml stacking gel buffer

   4 ml 10% SDS

   2 ml glycerol

   1 ml β-mercarpoethanol

   35 µg bromophenol blue

Made up to 10 ml with dH_2O.

10. 10X TBS (pH=7,4)

10 g NaCl

30 g Tris

2 g KCl

Made up to 1 L with dH_2O.

This was diluted to 1X and used for TBST with 0.05% Tween-20

11. 10X TBST for β-actin antibody (pH=7,4)

80 g NaCl

2 g KCl

30 g Tris

10 ml Tween-20

Made up to 1 L with dH_2O.

12. TBS-BSA

0,5 g BSA in 100 ml of TBS

A2.5 Polyacrylamide gels

Table 6: Polyacrylamide Gel Recipe for two gels

Reagent	**12,5% Separating Gel**	**4% Stacking Gel**
Monomer Solution	6,25 ml	940 µl
Separating gel buffer	3,75 ml	0
Stacking gel buffer	0	1,75 ml
10% SDS	150 µl	70 µl
Distilled water	4,75 ml	4,3 ml
Initiator Reagent (APS)	75 µl	35 µl
TEMED	15 µl	15 µl

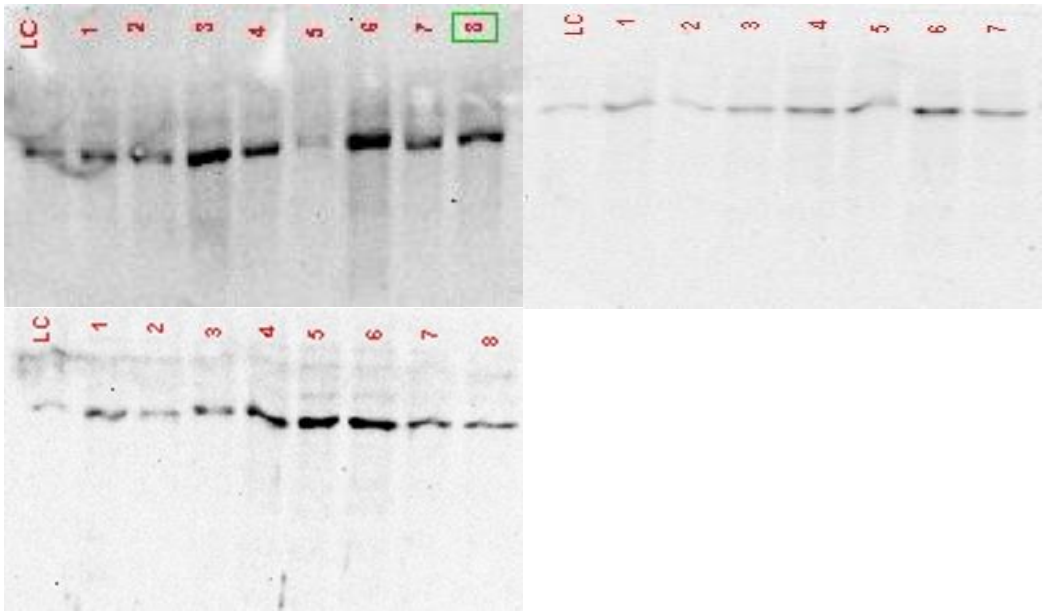
A3 Statistical Analysis: T-tests vs ANOVA

CNP	**t-test p-value**	**ANOVA**
Saline vs ibogaine	>0,9999	0,7128
saline vs morphine	0,3065	0,2537
saline vs MI	0,001	0,003
saline vs MI2	0,2286	0,7407
MI vs MI2	0,0051	0,0086
MBP	**t-test p-value**	**ANOVA**
Saline vs ibogaine	<0,0001	0,0277
saline vs morphine	0,7994	0,8931
saline vs MI	0,0381	0,1939
saline vs MI2	0,0411	0,0439
MI vs MI2	0,2714	0,4175
PLP	**t-test p-value**	**ANOVA**
Saline vs ibogaine	0,0003	0,0657
saline vs morphine	0,0006	0,0141
saline vs MI	0,4413	0,6468
saline vs MI2	<0,0001	0,0189
MI vs MI2	0,0267	0,061

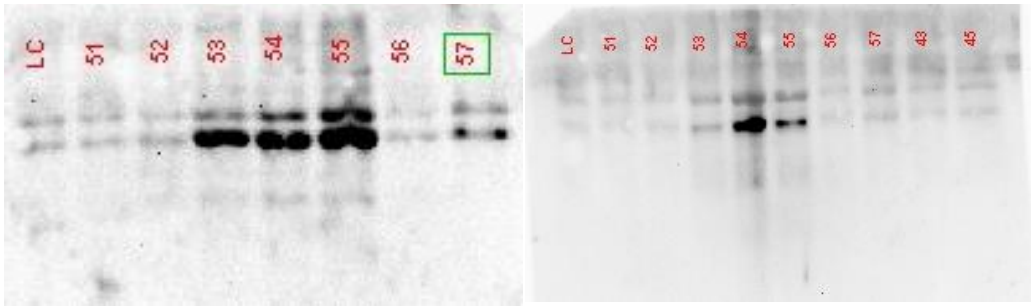
A4 Western Blots

A4.1 Actin

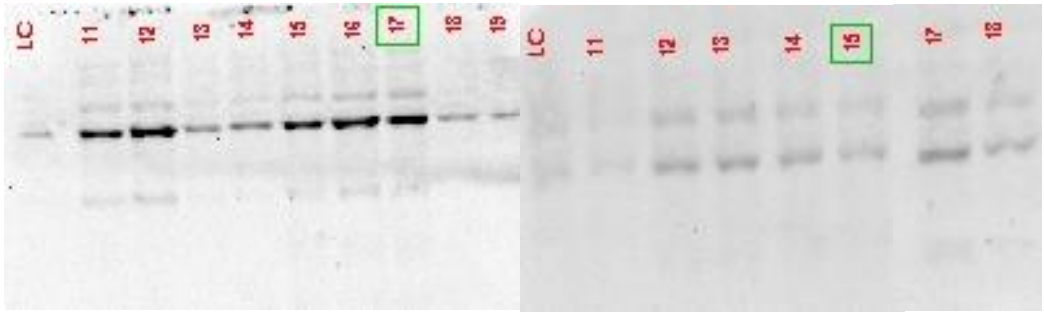
Saline control western blots with repeats



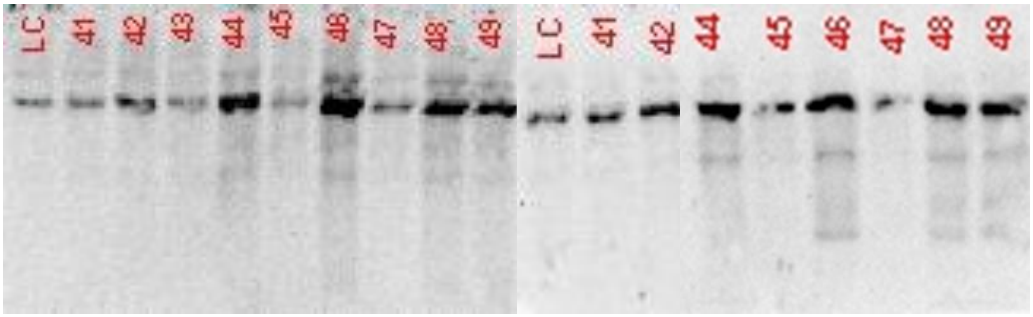
Morphine control western blots with repeats



Ibogaine control western blots with repeats



Morphine Ibogaine western blots with repeats



Morphine Ibogaine 2 western blots with repeats

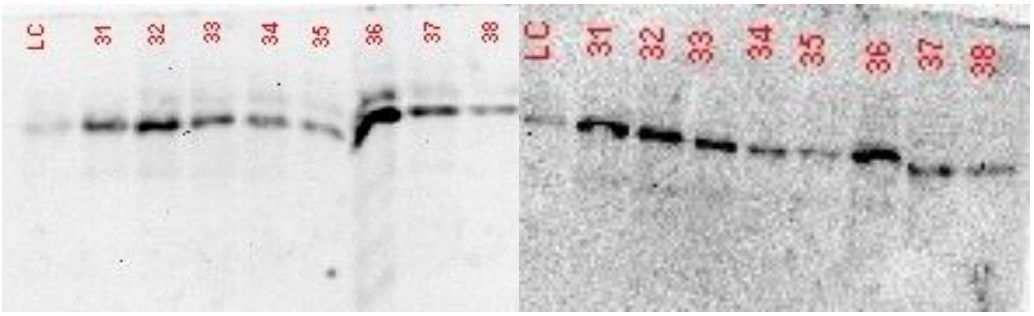
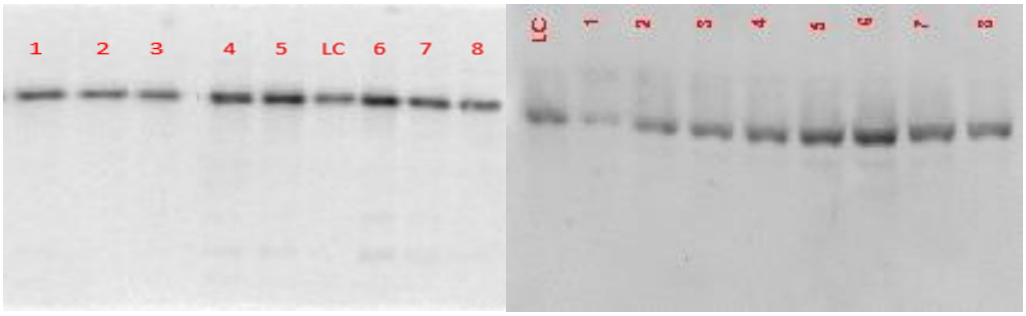


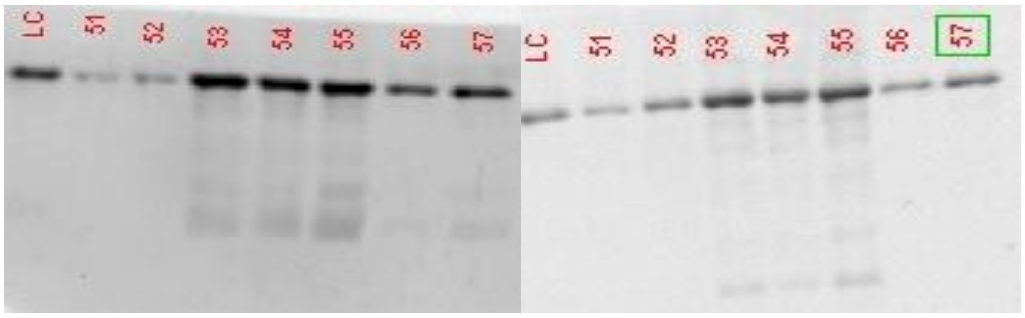
Figure 16: Beta actin probed immunoblots with repeats

A4.2 CNPase

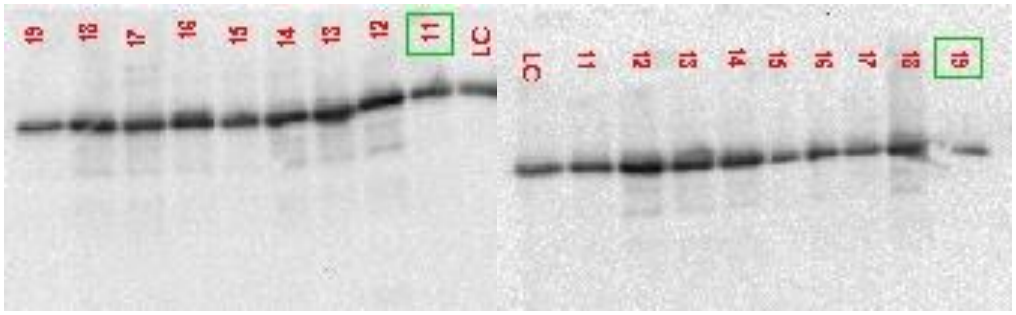
Saline Control western blots with repeats



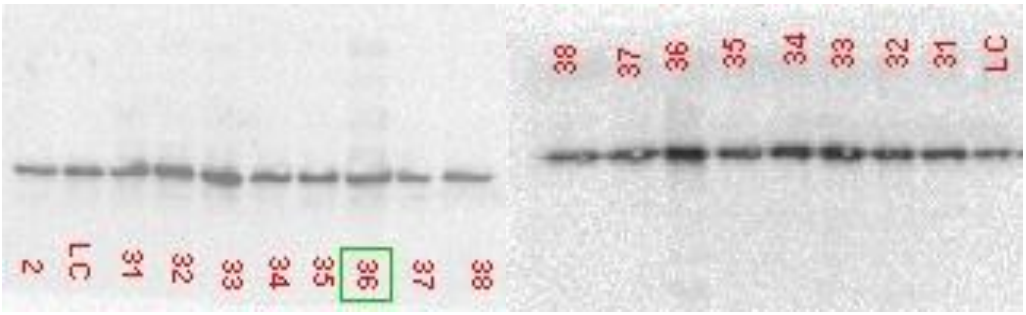
Morphine Control western blots with repeats



Ibogaine Control western blots with repeats



Morphine Ibogaine western blots with repeats



Morphine Ibogaine 2 western blots with repeats

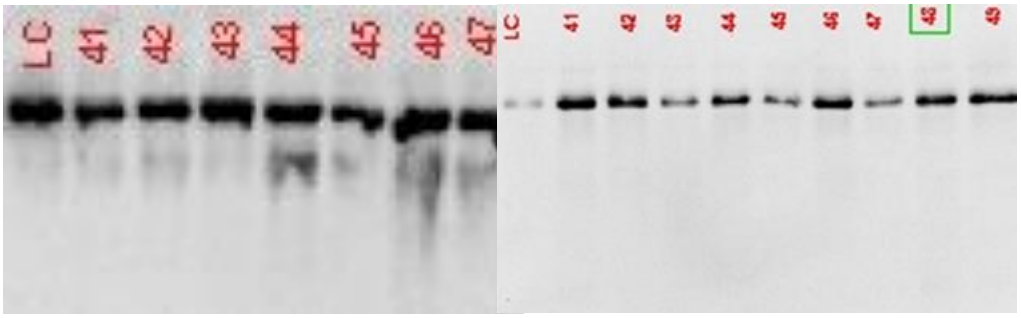
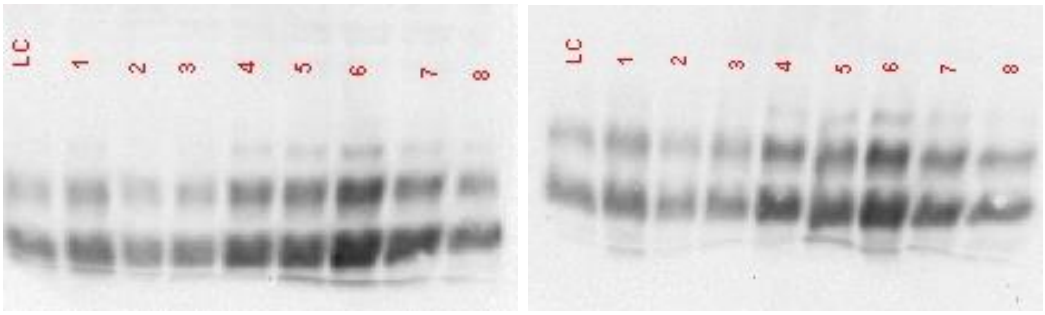


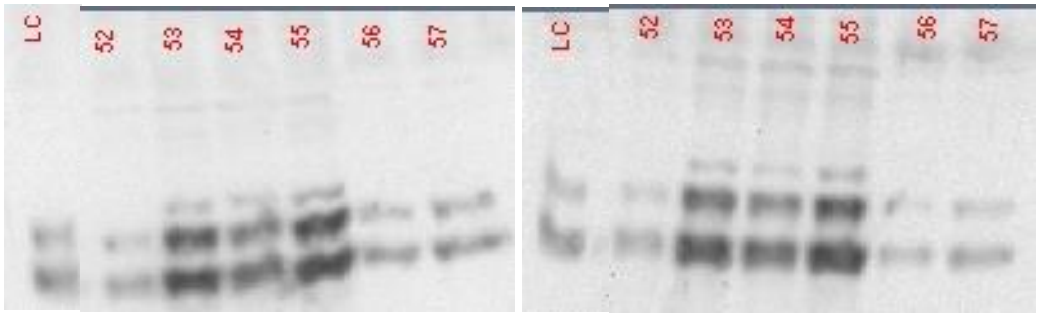
Figure 17: CNPase probed immunoblots with repeats

A4.3 Myelin Basic Protein

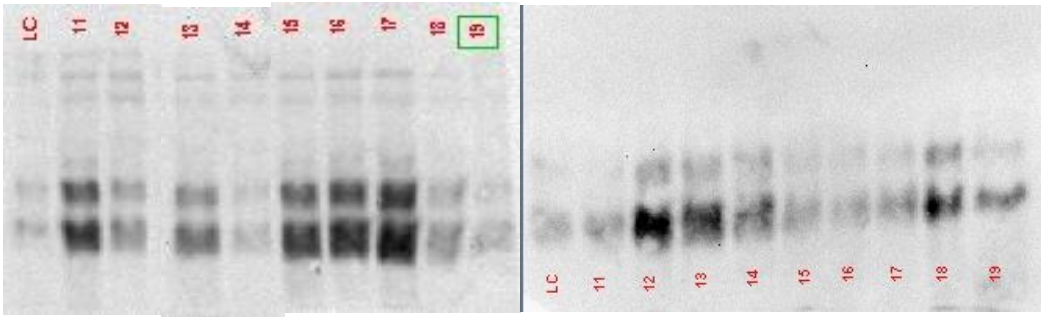
Saline Control western blots with repeats



Morphine Control western blots with repeats



Ibogaine Control western blots with repeats



Morphine Ibogaine western blots with repeats



Morphine Ibogaine 2 western blots with repeats

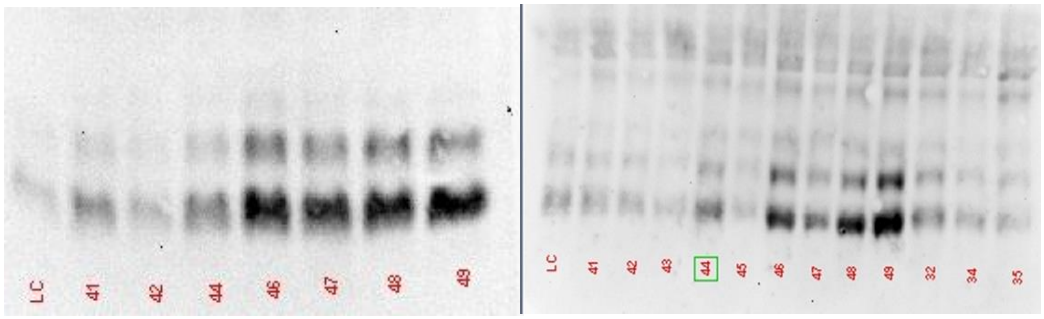
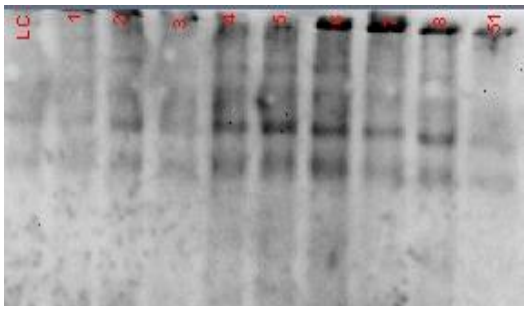


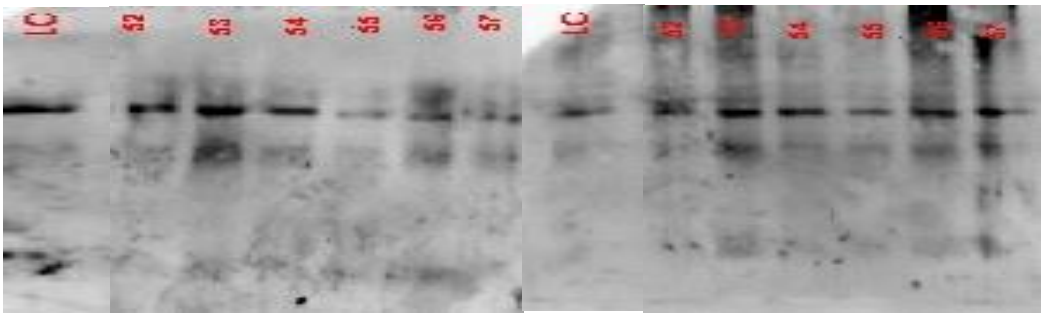
Figure 18: MBP probed immunoblots with repeats

A4.4 Proteolipid Protein

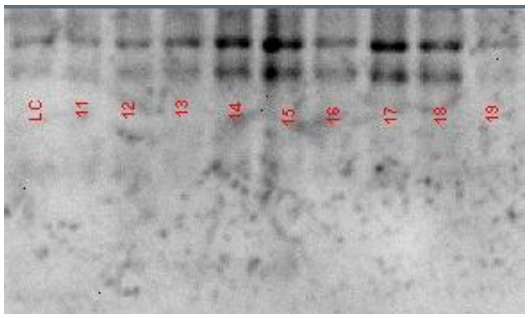
Saline Control western blot



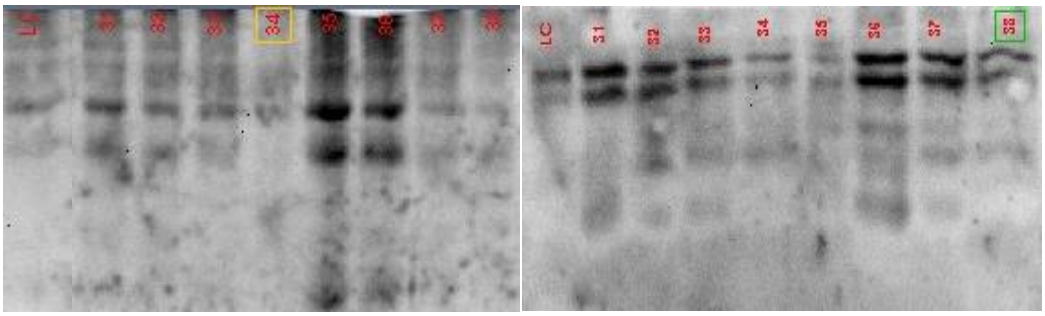
Morphine Control western blots with repeats



Ibogaine Control western blot



Morphine Ibogaine western blots with repeats



Morphine Ibogaine 2 western blots

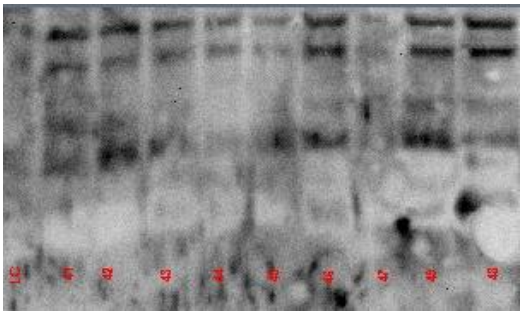


Figure 19: PLP probed immunoblots with repeats

A5 Additional qPCR Results

Table 8: data on standard curves of qPCR data

Gene	Group	Slope	Efficiency	R^2	Error	Y-intercept
CNP	Saline control	-2,2354	2,8	1	0,07	18,65
	Ibogaine control	-2,1353	2,94	1	0,1	18,78
	Morphine control	-2,1503	2,92	1	0,11	18,8
	Morphine ibogaine 1	-2,5037	2,51	0,95	0,68	21,58
	Morphine ibogaine 2	-2,1637	2,9	1	0,12	18,89
MBP	Saline control	-3,9386	1,79	0,96	1,34	35,51
	Ibogaine control	-3,8243	1,83	0,97	1,08	33,95
	Morphine control	-5,8324	1,44	0,94	1,92	38,82
	Morphine ibogaine 1	-5,5663	1,51	0,96	1,39	35,24
	Morphine ibogaine 2	-5,5211	1,52	0,94	2,06	37,06
PLP	Saline control	-3,5167	1,92	0,95	0,74	28,67
	Ibogaine control	-3,2324	2,04	0,95	0,97	28,11
	Morphine control	-4,3273	1,70	0,97	0,91	26,40
	Morphine ibogaine 1	-5,246	1,55	0,94	1,64	30,90
	Morphine ibogaine 2	-4,8423	1,61	0,96	1,18	28,41

Table 9: Fold change of CNP mRNA expression relative to saline control

Treatment group	**Fold Change ($E^{-\Delta\Delta Cq}$)**
Morphine control	4,856
Ibogaine Control	2,023
Morphine Ibogaine 1	6,453
Morphine Ibogaine 2	1,734

Table 10: Fold change of MBP mRNA expression relative to saline control

Treatment group	**Fold Change ($E^{-\Delta\Delta Cq}$)**
Morphine control	1,075
Ibogaine Control	0,2227
Morphine Ibogaine 1	2,009
Morphine Ibogaine 2	2,960

Table 11: Fold change of PLP mRNA expression relative to saline control

Treatment group	**Fold Change ($E^{-\Delta\Delta Cq}$)**
Morphine control	0,2132
Ibogaine Control	5,043
Morphine Ibogaine 1	0,8443
Morphine Ibogaine 2	0,3189